Received: 30 March 2023 | Revised: 20 April 2023 | Accepted: 9 May 2023 | Published online: 10 May 2023

REVIEW

Archives of Advanced Engineering Science
2024, Vol. 2(1) 1–23
DOI: 10.47852/bonviewAAES3202915

BON VIEW PUBLISHING

A Review on Recent Achievements and Challenges in Electrochemical Machining of Tungsten Carbide

Mohammed Asmael[1],* and Amin Memarzadeh[2]

[1]*School of Mechanical and Aerospace Engineering, Queen's University Belfast, UK*

[2]*Department of Mechanical Engineering, Eastern Mediterranean University, Türkiye*

Abstract: Electrochemical machining (ECM) is a modern, unconventional manufacturing technique that uses the electrochemical dissolution of metal to produce pieces with a predetermined shape, dimensions, and surface polish. Tungsten carbide (WC) is used in many fields and applications due to its high wear resistance and hardness. WC is used in cutting tools, mining and drilling equipment, wear parts, industrial machinery, aerospace and defence components, and medical equipment. It gives a workpiece a particular shape and number of boreholes, removes a damaged outer coat, and eliminates surface roughness. Though the ECM of WC is fraught with difficulties and obstacles, altering the electrolytes and refining the technological equipment and process of the ECM of WC can help improve machining accuracy and stability. In the current study, we examined the ECM of WC and compiled a reliable database from reliable sources using the keywords "electrochemical machining" and "tungsten carbide". Research papers constitute the majority of these publications. It was discussed how WC behaves anodically as it applies to ECM, which experiments were conducted with various electrolytes, and how they performed. Several ECM modes have been considered, and each mode has been evaluated in detail for challenges and gaps.

Keywords: electrochemical machining, electrochemical shaping, manufacturing, tungsten carbide, anodic dissolution, electrolytes

1. Introduction

In the aerospace, automotive, electronics, medical devices, optical, and communications sectors, macro- and micro-product demand and mechanisms for challenging materials, like super alloys, tool steel, carbides, and titanium alloys, are quickly increasing. Despite their unique features, several machine-intensive materials are in short supply (Rajurkar et al., 2013). These materials present various problems for typical machining operations like turning and milling. Electrochemical machining (ECM) is a modern unconventional manufacturing technique that uses the electrochemical dissolution of metal to produce pieces (Davydov & Kozak, 1990; Davydov et al., 2004; Davydov et al., 2017; De Barr & Oliver, 1968; McGeough, 1974; Shmanev et al., 1986; Wilson, 1971). ECM is a collection of procedures that give a workpiece (WP) (such as a die block or turbine blade) a particular shape using anodic dissolution, bore holes into it (blind, though, with curved axes of varying cross-section), remove a damaged outer coat from it (ECM without shaping), certify a defined degree of surface roughness, and eliminate it (Davydov et al., 2004). This technique produces parts with predetermined figures, dimensions, and surface polish (Wang et al., 2023; Xu et al., 2023).

A concentrated electrolyte flow is created to clear the working zone of the by-products of electrochemical and potential chemical processes and replenish the electrolyte composition there. The simple idea is that a perfect anodic dissolution occurs in extraordinarily conductive electrolytes at high densities of current ranging from 5 to 100A cm^2 (Bannard, 1977; Datta, 1993). Figure 1 (Arafat & Fanghua, 2020) illustrates one kind of ECM involving a tube-shaped tool electrode to create a dump with a spherical cross-section (TE). TE is gradually incorporated into the WP at a rate equal to the metal dissolving rate at the bottom of the hole to form a hole. As a result, the machining gap (SF) (interelectrode distance) is maintained constant. The interelectrode spacing should typically be smaller than 100 μm to increase TE replication's precision on the WP.

Due to its unique characteristics, tungsten carbide (WC) is helpful in many fields and applications. WC is widely used in cutting tools such as drills, saw blades, and milling cutters because of its high wear resistance and hardness. WC is used for producing mining and drilling equipment such as drill bits, cutting tools, and mining machinery parts. Due to its high resistance to wear and corrosion, WC is used in worn parts such as nozzles, valve seats, and pump seals. WC is used to produce industrial machinery components such as gears, bearings, and seals. WC is used to produce aerospace and defence components such as armour-piercing projectiles, missiles, and engines. WC is used to produce medical equipment such as dental drills, surgical instruments, and prosthetic implants due to its biocompatibility and hardness.

ECM's benefits and drawbacks are well examined in the literature (Davydov et al., 2004; Davydov & Kozak, 1990; De Barr & Oliver, 1968; McGeough, 1974; Shmanev et al., 1986; Wilson, 1971). Mineral salt aqueous solutions (NaCl, $NaNO_3$, and KBr) are

*Corresponding author: Mohammed Asmael, School of Mechanical and Aerospace Engineering, Queen's University Belfast, UK. Email: m.asmael@qub.ac.uk

Figure 1
Diagram of tubular electrode-tool, insulation, and important zones in the electrochemical machining process

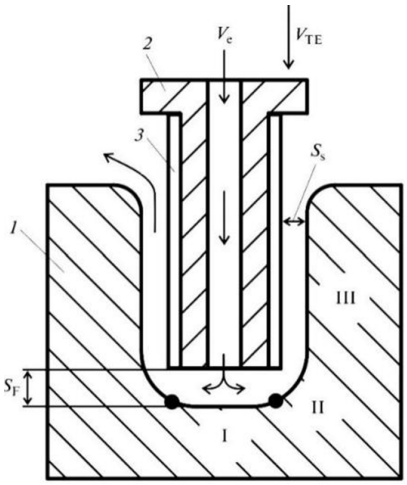

commonly employed in ECM. Nevertheless, more harsh electrolytes (acid combinations) are utilised in alternative approaches to metal electrochemical treatment (etching and polishing) (Davydov et al., 2017). Many ECM detailed structures depend on the kind of WP, the desired operation, and the skill employed. Many papers have been dedicated to general issues with multiple ECM techniques of different metals. Studies about the ECM of WC are focused on, and the electrochemical features of tungsten carbide in the ECM process are considered, which form the foundation or are primarily considered while creating various ECM methods.

2. Methodology

In this review article, the database of articles comprised three reliable sources: Scopus, ScienceDirect, and Google Scholar. The articles were searched according to these keywords: "electrochemical machining" or "ECM" and "tungsten carbide" or "WC". Figure 2 (Scopus, n.d) displays the total 65 collected sources published from 1972 to 2022. Most of these publications were research papers, accounting for more than 32%; conference papers, accounting for about 2%; and review papers, accounting for less than 2%. Recent articles related to the ECM or WC were added to the sources for a better perspective. Figure 3 (Scopus, n.d) provides more information about the database used.

3. Properties of Tungsten Carbide

WC defines as tungsten beside carbon atom-based chemical compound. With a modulus of Young between 530 and 700 GPa (Blau, 2003; Cardarelli, 2001; Groover, 2020; Kurlov & Gusev, 2013) and a concentration that is roughly halfway between gold and lead concentrations, it is roughly double as inflexible as steel. In terms of rigidity, it is comparable to corundum (α -Al_2O_3). Factually, WC is known as Wolfram. The composite material known as "tungsten carbide" was made by carburising wolframite ore and cementing it with a binder (Helmenstine, n.d.). In Swedish, the word "tungsten" denotes a heavy stone. Table 1 lists some of the significant characteristics of WC. Carbon and tungsten metals react to produce WC at temperatures ranging from 1400 to 2000°C (Pierson, 1999). Alternative methods include a fluid bed process that uses tungsten metal or blue WO_3 and CO/CO_2 and H_2 at temperatures between 900 and 1200°C (Lackner & Filzwieser, 2002). WO_3 can also be directly heated with graphite at 900°

Figure 2
Published documents per year with keywords "electrochemical machining", "ECM", "tungsten carbide", and "WC"

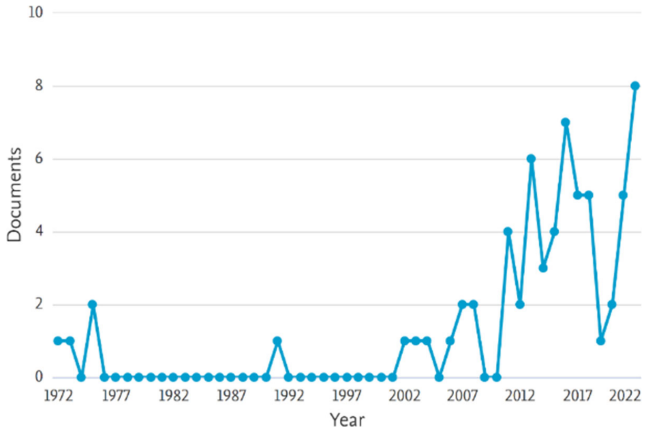

Figure 3
Distribution of published documents by type and with keywords "electrochemical machining", "ECM", "tungsten carbide", and "WC"

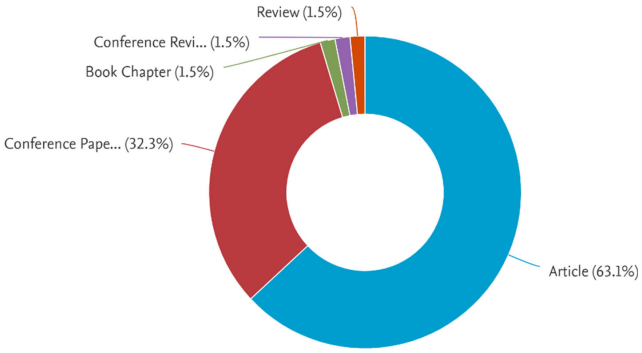

Table 1
Basic characteristics of tungsten carbide

Formula	WC
Appearing	Grey-black glossy solid
Molar mass (g.mol^{-1})	195.85
Point of melting (°C)	2785–2830 (Pohanish, 2012; Song & Williams, 1993)
Density (g.cm$^{3)}$	15.63
Point of boiling (°C)	6000 at 760 mmHg (Pohanish, 2012)
Solubility	Soluble in HNO_3, HF (Song & Williams, 1993)
Conductivity (thermal; W.m^{-1}.K^{-1})	110 (Blau, 2003)
Magnetic susceptibility (χ; cm3.mol^{-1})	1·10 − 5 (Song & Williams, 1993)

C or hydrogen at 670°C before being carburised in argon at 1000°C to produce WC (Zhong & Shaw, 2011). Superbly powdered WC willingly rusts in aqueous hydrogen peroxide solutions (Nakajima et al., 1999). The tungsten semi-carbazide, W_2C, and WC are well-known tungsten and carbon compounds (Jacobs et al., 1998). Other metastable carbon and tungsten compounds are produced via quenching the WC phase in an inert gas after heating it to a high temperature (plasma spheroidisation) (Károly & Szépvölgyi, 2005). WC decays to carbon and tungsten at high temperatures, as can happen using thermal spraying procedures at high temperatures like High-velocity oxygen fuel (HVOF) and High-energy plasma (HEP) (Nerz et al., 1992). The oxidation of WC begins around 500–600°C (Pierson, 1999). WC is acid resistant and is only attacked above the room's temperature through mixtures of HF/HNO_3 (Pierson, 1999). It interacts with chlorine above 400°C and fluorine gas at average temperature but is inert to dry H_2 up to its melting point (673 K) (Pierson, 1999). With a bulk modulus of 630–655 GPa and a shear modulus of 274 GPa (Kurlov and Gusev, 2013), WC is tough. It has a ratio of Poisson of 0.31 and about 2.7 GPa maximum compression strength (Kurlov and Gusev, 2013). A longitudinal tendency travels over a WC rod at 6220 $m.s^{-1}$ (Cafe, n.d.). WC has a small electrical resistivity of around 0.2 m, equivalent to some metals (for instance, 0.2 μΩ·m for vanadium) (Kittel & McEuen, 1996). Cobalt and molten nickel readily wet WC (Ettmayer & Walter Lengauer, 1994). WC has two structures: hexagonal form, α-WC (Kurlov & Gusev, 2013; Wells, 2012), and cubic high-temperature form, β-WC, which has a rock salt structure (Sara, 1965). The hexagonal form comprises a simple hexagonal frame of metal atoms of layers lying directly over one another, with carbon atoms filling half the spaces, giving both tungsten and carbon a regular trigonal prismatic, 6 coordination (Wells, 2012). Using the measurements of a unit cell, the following bond lengths can be determined (Rudy et al., 1962): The shortest distance between tungsten atoms in adjacent layers is 284 pm, the tungsten carbon bond length is 220 pm, and the distance between tungsten atoms in a hexagonally packed layer is 291 pm. Similar to the single bond in $W(CH_3)_6$, the tungsten–carbon bond is similar in length (218 pm) (Kleinhenz et al., 1998). Molecular WC has been studied, and the bond length for 184W12C in the gas phase is 171 pm (Sickafoose et al., 2002).

4. Overview of Reviewed Sources

WC's formidable hardness poses challenges for conventional machining, prompting exploration into innovative techniques like jet electrochemical molding (Jet-ECM). In studies by Hackert-Oschätzchen et al., Jet-ECM emerges as a pivotal method for precise micromachining. The first study (Hackert-Oschätzchen et al., 2013b) delves into micro-patterning, demonstrating localized material removal using the continuous, direct current to craft point or line microstructures. The second study (Hackert-Oschätzchen et al., 2013c) focuses on microstructuring carbide metals, underscoring Jet-ECM's precision and enhanced dissolution rates compared to pulsed electrochemical processes. In the subsequent investigation (Hackert-Oschätzchen et al., 2013a), the closed-loop jet ECM approach selectively removes metal from WC surfaces, creating intricate microstructures and three-dimensional patterns. Jet-ECM stands out as a promising solution for tackling the hardness of WC, offering precision in intricate microfabrication.

Instead of the more usual alkaline solution used in WC electrochemical processing, Liu et al. (2015) study Electrochemical slurry jet micro-machining (ESJM) of WC utilising a pH-neutral NaCl electrolyte. Yang et al. (2017) propose a sliding electrochemical machining method to fabricate WC micro fins. Zhang et al. (2018) look into using electrochemical processing and ultrasonic vibration to lessen diamond tool wear during WC machining. It is suggested to use a hybrid approach to incorporate the electrochemical surface treatment of the WC WP into the diamond turning process. Wang et al. (2019) evaluated the viability of a method for recovering cobalt and tungsten by transforming solvable compounds into unsolvable ones. They employed the method to recover tungsten as $CaWO_4$ and cobalt as CoH_2O. Geethapriyan et al.'s (2019) main goal is determining Metal removal rate (MRR), surface roughness, and overcut when machining WC in EMM using sodium nitrate ($NaNO_3$) as an electrolyte. Joseph et al. (2022) intend to spur the production of various advanced hierarchical structures using a straightforward hydrothermal method with many possible uses. Using the electrical discharge machining (EDM) of ultrafine particles of WC, Gattu and Yan (2022) observed single discharge craters and hole machining performance to investigate the effects of mixing insulative alumina powder (Al O), semiconductive silicon powder (Si), and electrically conductive carbon nanofiber (CnF) at various focusses in dielectric fluid. The principal objectives of Awaludin et al. (2022) are to investigate the performance of temperature distribution and equivalent Von-Mises stress development on WC, to ascertain the impact of various machining parameters on the WC WP, to make a group of constraints, temperature dispersal, and stress expansion which can be likened with the investigational results, and to optimise the machining parameters for wire EDM of WC. Yan et al. (2022) present a method for creating practical and durable bimetallic carbide composites as better electrocatalysts and electrode materials. Feng et al. (2022) investigate the potential of profound importance for low-valence tungsten reduction to prevent disproportionation reactions in molten alkali chlorides. Wang et al. (2022) suggest a novel hybrid machining technique called photocatalytic-assisted jet electrochemical machining to enhance machining capacity by simultaneously removing the metal aluminium matrix and the SiC particles. Aseerullah et al. (2022) use ANSYS software to analyse the CNC machining procedure of AA6082-T6.

The testing and analytical findings are used to validate the task. Kode et al. (2022) investigate laser-aided diamond turning of WC and the material characteristics needed to achieve an optical surface finish appropriate for lens moulds. The machinability of five grades of WC specifically created for glass lens moulds was investigated. Sun et al. (2022) suggest a two-step rapid reciprocating etching technique for producing Liquid metal ion source (LMIS) tungsten needles with variable tip length, apex radius, and a smooth transition area between the needle tip and the needle shaft. Other outstanding studies include Kokulnathan et al. (2023) and Ratnasingam et al. (2009). As mentioned in the methodology section, the total number of collected articles according to the keywords: "electrochemical machining" or "ECM" and "tungsten carbide" or "WC" was 65, but to have a better perspective, recent articles related to the ECM and recent articles related to WC added to sources. An overview of reviewed articles is available in Table 2.

5. How WC Behaves Anodically in ECM

Several electrolyte combinations are documented in the literature. In this part, we will go through the current state of the art and analyse the benefits and drawbacks of each electrolyte. Anodic dissolution is essential for material modification in the ECM technique. In a fastened circuit, the electrolyte is stimulated to dissolve. The products cannot be eliminated by diffusion due to the high current densities of up to 100 A cm^2 but instead form supersaturated surface layers (Lohrengel & Rosenkranz, 2005). Several systems, including Al, Cu, Cr, Fe, Mn, Mg, V, Ni (Münninghoff, 2011), and numerous compounds, have previously been investigated. This testing resulted in the development of several regulations. Because nearly all essential metal nitrates crystallise extremely gradually, between flashes or days, the rising quantity of corrosion cannot be eliminated by diffusion, and

Table 2
An overview of reviewed sources

Questions focus	Materials workpiece electrolyte	Operations modes	Outcomes findings	Refs.
Niobium carbide micro-EDM milling nickel	• NbC-12Ni	Micro-EDM	Micro-EDM technology has optimised the machining process for NbC matrix ceramics	(Ye et al., 2022)
WC–Co micro-tools for micromachining using an environmentally friendly electrolyte	• WC–Co • NaOH • $NaNO_3$ • H_2SO_4 • $NaNO_3 + C_6H_8O_7$	Micro-WECM	Micro-WECM is utilised to anode WC–Co alloy utilising four distinct electrolytes via micro-tool manufacturing	(Sethi et al., 2022)
The Importance of waveform design	• Nb • H_2SO_4–HF	Jet-ECM	Bipolar-EJM can be used to machine passivation-sensitive materials	(Xue et al., 2022)
Machining characteristics	• NbC without WC • NbC with WC • 20% $NaNO_3$	Micro-ECM	The machinability of two grades of NbC	(Arshad et al., 2022)
Wear of electrode tool	• WC alloy • $NaNO_3$ aq. 5 wt%	Bipolar pulse ECM	A novel bipolar nanosecond pulse power supply successfully manufactured micro holes	(Zhang et al., 2022)
Inconel 718 machinability	• Inconel 718	Review	A rigorous examination of the effect of reducing temperatures	(Mahesh et al., 2021)
Simulation of electrochemical micromachining machining parameters	• 316L	3D simulation	Experiments are used to validate simulation findings, resulting in a 15% variance from experimental results	(Kumar et al., 2021)
Electrolyte solution suitable for anodic dissolution	• Nickel • Aluminium bronze • $NaNO_3$ • NaCl	Micro-ECM	The machining properties of two grades of NAB are investigated	(Palani et al., 2021)
Oxide film formation prevents material dissolution under low current density	• Ti-6Al-4V, • Inconel 718 • 15 wt% NaCl aq.		Experiments using a suction tool validated the suggested model and instructions	(Hizume & Natsu, 2021)
Micro-hole drilling	• (SS-316L)	ECMM	Material removal rate, overcut, and conicity increase as machining voltage increases	(Dutta et al., 2020)
Tool electrode feed rate affects ECDD	• Glass	ECDD	TEFR has been found to influence the geometric properties of micro-holes in glass created by velocity-feed ECDD	(Arab & Dixit, 2020)
MRR and dimensional deviation are affected by process factors	• Nimonic 75 • WC as the tool	TOPSIS	Lower duty cycle and pulse levels are preferred for improved geometrical properties	(Shamli et al., 2020)
The ECMM parameters impact the rate of material removal and electrode wear	• Hybrid Al/(Al_2O_3p+SiCp +Cp)-MMC • Tungsten electrode of diameter 298 μm	ECMM	Micro-sparking at high voltage and pulse on time deposits hybrid metal matrix composite on a micro tool owing to melting and re-solidification during machining	(Kalra, et al., 2020)
NAB alloy may be anodised by electrochemical micromachining	• Nickel • Aluminium bronze • $NaNO_3$ • NaCl	Micro-ECM	The CCD-RSM technique was used to quantify radial overcut, material removal rate, and surface roughness, demonstrating the appropriateness of electrode materials for the micromachining of nickel aluminium bronze alloy	(Palani et al., 2020)
Machining with a magnetic field and electrochemical discharge	• Platinum • WC rod • Potassium hydroxide	ECDM	The gas film state dramatically impacts the processing outcome, and by limiting it, the processing range and accuracy may be enhanced	(Lin et al., 2019)

EMM performance is studied using WC	• WC • $NaNO_3$	EMM	The optimal settings for EMM of WC include an electrolyte concentration of 20 g/l, tool feed rate of 0.9 μm/min, and voltage of 9 V	(Geethapriyan et al., 2019)
The engraving is done on soda lime glass	• WC • Soda-lime glass material • KOH	ECDM	Tool rotation speed and feed rate breadth affect HAZ and OC changes	(Harugade et al., 2019)
ECMM with WC microfabrication on 17-4 PH SS alloy	• 17-4 PH stainless steel • Different electrolytes	ECMM	$NaCl+NaNO_3$ electrolyte enhances material removal rate, radial overcut, surface integrity, and dimple depth	(Thakur et al., 2019)
Mixed alkaline electrolytes increase machining efficiency	• (WC) tool • NaOH + KOH	ECDM	Deeper microchannels with sharper sidewalls were created using 25, 30, and 35 wt% mixed electrolytes, but in the attendance of salt electrolytes, poor MRR and surface quality were created due to low energy and dangerous electrochemical sparks. WC used in NaOH and $NaNO_3$ exhibited extra severe wear and erosion of the tool.	(Sabahi & Razfar, 2018)
The hybrid approach combines electrochemical surface treatment of the WC workpiece with diamond turning	• WC • Polycrystalline diamond tools	Combination of ultrasonic vibration and electrochemical processing	Compared to ultrasonic vibration cutting without electrochemical processing, the proposed hybrid approach may greatly minimise diamond tool wear and enhance the surface quality of machined ultra-fine grain WC workpieces	(Zhang et al., 2018)
Features of drilling of micro-hole	• WC–Co • NaOH	Micro-ECM	Desktop micro-ECM can make micro-holes in WC–Co workpieces	(Wu & Sheu, 2018)
Micro-hole drilling	• Tungsten cemented carbide • H_2SO_4	Micro-ECM	ECM drilled micro holes employing incredibly brief voltage pulses to drill stainless steel sheets using WC tool electrodes	(Egashira et al., 2018)
Grinding of wire electrochemically	• Tungsten rod • $NaNO_3$	WECG	WECG was proposed for machining micro-rods of tungsten with a (diameter=35μm and length=163μm) without tool wear because of bipolar current	(Han & Kunieda, 2018)
Electrode fabrication for microhole machining.	• Pure aluminium ingot	Hot dip aluminising micro-arc oxidation	The electrode insulation has reduced the stray effect and achieved high-precision machining	(Hung et al., 2018)
Create micro-hole profiles	• Nimonic 75 • WC • Sodium bromide • Hydrofluoric acid • Ethylene glycol • Sodium chloride • $NaNO_3$	Electrochemical micromachining	According to experimental findings, the second electrolyte provides a faster material removal rate, whereas the first electrolyte produces lower values of overcut and conicity	(Pillai et al., 2017)
Sintered alloy microstructures and characteristics are compared	• WC–HEA • WC–Co-cemented carbide	Electron microscope X-ray diffraction mechanical property and electrochemical testing	Cemented carbides based on WC with ultrafine grains can be bound with AlFeCoNiCrTi HEA, improving mechanical properties and corrosion resistance	(Zhou et al., 2017)
ECM is employed to process sintered carbide at high speeds	• Sintered • Carbide with Iron Ions • NaCl and FeCl2	ECM	Fe2+ ions prevent excessive cobalt elution from a sintered carbide workpiece during ECM	(Wang et al., 2017)

(*Continued*)

Table 2
(*Continued*)

Questions focus	Materials workpiece electrolyte	Operations modes	Outcomes findings	Refs.
Make tiny fins out of WC	• WC • $NaNO_3$ • Sodium hydroxide	Sliding electrochemical machining (SECM)	A quick sliding workpiece and a pulse power source can be used to fabricate micro-fins	(Yang et al., 2017)
Microrelief was created by dissolving the WC25 coating using electrochemistry	• WC25 • 10%$NaNO_3$	Electro diamond grinding	The WC chipping caused by the WC25 electro-diamond grinding can improve the coating by turning off the source of technical current	(Burov et al., 2016)
To finish difficult-to-machine materials, ECMP employs fixed abrasive grain	• SiC, WC, and GC	ECMP	Slurry-less ECMP was achieved due to low anodic oxidation potential	(Yamamura et al., 2016)
Electrode insulation layer fabrication for ECM	• WC tool	Hot dip aluminising micro-arc oxidation	The electrode is designed to reduce ECM effects and improve mould cavity accuracy	(Hung et al., 2016)
Sintered carbide ECM phenomena	• Sintered carbide • NaCl	ECM	The mid-link machining current, machining speed, and surface quality were examined	(Goto et al., 2016)
Pulse parameters influence the form of straight-lined grooves	• WC6Co • $NaNO_3$ • NaOH	Jet-ECM	By organising corresponding line deletions in Jet-ECM with the pulsed current, waviness can be manufactured in WC6Co	(Martin et al., 2016)
Creating a pulse power supply to fulfil μECM requirements	• WC–Co • A mixture of sulphuric acid and $NaNO_3$	Micro-ECM	Micro-tools made with 170 μm WC–Co alloy shafts and μECM	(Spieser & Ivanov, 2015)
ESJM of WC	• WC • PH-neutral NaCl	ESJM	ESJM has the ability to mill difficult-to-cut metals, resulting in increased corrosion rate, current density, and localisation of machining	(Liu et al., 2015)
Inconel 718 ECG	• Inconel 718 • $NaNO_3$	ECG	Inconel 718 has distinct grinding properties	(Qu et al., 2015)
Micro-drilling	• Pyrex type glass	Chemical engraving spark assisted	Tool wear, drilling time, and contact force all impacted processing performance.	(Gao et al., 2014)
Using ultra-short pulses, the ECM of WC with WC–Co	• WC–CO • $NaNO_3$ • H_2SO_4	micro-ECM	A combination of $NaNO_3$ and H_2SO_4 was discovered to be optimum for the micro-ECM of WC	(Choi et al., 2013)
Create a feedback-controlled PECMM system for electrochemical WC micromachining	• WC	PECMM	A feedback-controlled PECMM system was created to improve the electrochemical micromachining of WC due to the increased interelectrode gap	(Kamaraj et al., 2012)
A unique pulsed power generator is employed to back nanosecond pulses in drilling	• WC pin • Nickel plates	ECMM	Working factors like the applied voltage, pulsed duration, electrolyte concentration, tool feed rate, pulse frequency, and hole depth affect the hole, conicity, and overcut	(Fan et al., 2012)
Water spray ED-drilling to prevent rusting	• WC–CO	ED-drilling	Water spray settings of 1500 ml/min and 60 ml/min were used to machine electrolytic-corrosion-free holes on WC–Co	(Song et al., 2012)
ECM manufacturing of micro-pins	• WC • $NaNO_3$	ECM	Micro-pins of WC alloy can be produced using $NaNO_3$ aqueous solution and ultrasonic cleaning, with a high electrolyte concentration and a lower machining current	(Shibuya et al., 2012)

Create tiny flow channels	• WC electrode • SUS316L	Micro-EDMM	Because of its faster reaction time and higher temperature, metallic-FC has a greater power density than graphite-FC	(Chang & Hung, 2011)
The diamond coating was applied on a cemented carbide substrate using a chemical vapour deposition process with direct current arc discharge	• WC–CO	Diamond coating	The time of electrolytic etching affects the quality and crystal characteristics of the diamond coating, with the surface shape changing from microcrystalline cubic-octahedron to cauliflower-type nanocluster as the etching duration increases	(Zhang et al., 2011)
Structural changes influence the electrochemical behaviour of doped electrodes	• Nano silicon/CMC/AB composite electrodes doped with WC	X-ray diffraction	By enhancing the mechanical qualities, WC doping can increase the cycle stability of nano silicon composite electrodes	(Wen et al., 2011)
The microstructure, mechanical, and electrochemical behaviour are affected by sintering settings	• WC-9%-Co containing 0.8%-Cr_3C_2 and 0.3%-VC	FAST	The influence of sintering temperature TS on mechanical, electrochemical, and reproducibility characteristics of sintered materials, the length-to-diameter ratio of cylindrical compressive samples and the effect of burrs created by electro-discharge machining was examined	(Krüger et al., 2011)
Surface micropatterning on bulk titanium (Ti)	• TI • WC tool	EMM	At high etch rates, pit and groove structures were created utilising a water-free electrolyte and a WC tool	(Sjöström & Su, 2011)
ECP can be used to improve machining parameters while spraying coatings	• HVOF	ECP+spraying coatings	With the proper machining settings, ECP can quickly reduce surface roughness from Ra=4.0μm to Ra=0.7μm	(Li et al., 2011)
Metallic bipolar plate manufacturing	• Tungsten electrode • SUS316L	Micro-EDM	Micro-EDM milling creates tiny flow channel shapes with a high aspect ratio for micro-PEM fuel cells	(Hung et al., 2011)
A rotating device collects insoluble sludge and fills it with electrolytes	• 304SS • $NaNO_3$ • WC pins	EMM	Micro-drilling was used to explore the effect of different factors on hole overcut and conicity	(Fan & Hourng, 2011)
Using WEDG, a tool electrode was made	• Quartz as workpiece • Tools: 304 Stainless steel • WC • Tungsten	WEDG	The surface roughness of a tool material determines the tool electrode wettability, which affects coalesce status, micro-hole diameter, and machining stability	(Yang et al., 2010)
Electrostatic microactuators enable the micro-electro-discharge method	• Copper as electrode • Stainless steels • WC–Co	A MEMS-enabled μEDM (M 3EDM) method	Electrostatic actuation of planar electrodes is used in μEDM	(Alla Chaitanya, et al., 2010)
Bipolar pulse and deionised water spray are used in WC-Co machining	• WC–Co	ED-milling	Spray ED milling produces high-quality micro-grooves with minimal corrosion and electrode wear	(Song et al., 2010)
An experimental material spinning disc was made on a high-speed lathe	• WC as tools • Oil palm, empty fruit bunches, and rubberwood • solid wood specimen	Material spinning disc	Tool wear is caused by separating hard carbide particles from the softened cobalt matrix	(Ratnasingam et al., 2010)
Micro-EDM uses a triangle electrode and a bipolar pulse power source to minimise electrolytic corrosion	• WC–Co	WEDG	They machined a corrosion-free electrolytic hole with deionised water and a bipolar pulse power source	(Song et al., 2009)
Using tungsten, copper, and silver electrodes provides a fine surface finish in micro-EDM	• WC as workpieces	Die-sinking μedm	AgW is the ideal material for WC finish die-sinking micro-EDM	(Jahan et al., 2009)

(*Continued*)

Table 2
(*Continued*)

Questions focus	Materials workpiece electrolyte	Operations modes	Outcomes findings	Refs.
Altering customary microtools	• WC	ECM Jet-ECM	WC can modify micro tools and operate with a free electrolyte jet	(Hackert et al., 2007)
Experiments in the production of WC micro-shafts	• WC rod • H_2SO_4	Electrochemical etching	An H_2SO_4 solution created a micro-shaft of WC with good straightness and surface superiority after 210 seconds of milling. Sludge was eliminated by submerging the shaft in a NaOH solution	(Choi et al., 2006)
Polycrystalline cathodes are used to treat cemented carbides	• Cemented carbides	EDMPC	Cemented carbides are machined using diamond-electrolytic technology and polycrystal cathodes with smooth working surfaces, resulting in an anomalous change in current density with electrode voltage rise	(Novikov & Gurvich, 2003)

supersaturated surface layers accumulate. These supersaturated films have unique features. They are alive, typically vividly coloured, and highly water soluble. They liquefy by electrolyte drive down to a few micrometres fixed values and ensure a polishing result. Since base metal chlorides crystallise significantly faster, slurries consisting of nanocrystals and solution development occur in most chloride solutions. As a result, the polishing effect is being abused. Water is transported to the surface partially via dispersal over these films; however, its action is minimal since practically. Every drop of water is utilised to hydrate cations.

$$2H_2O \rightarrow O_2 + 4H^+ + 4e^- \quad (1)$$

According to equation (1), oxygen evolution was focused on around one-fifth of the total charge and was counted by fluorescence extinction in several studies (Hammer et al., 2011).

5.1. Solutions of nitrate and chloride

Under potentiated circumstances, the anodal behaviour of the uncontaminated metals W and Co, the commercial sample WC/Co, and pure WC was examined using the flow-through tube cell. An ultraviolet-visible spectrometer was used to study the electrolyte at the capillary's exit in a flow-through cuvette. Walther et al. (2007) provide details on this well-established setup. Co wires and electropolished tungsten were also evaluated in conservative cells. Lohrengel et al. (2014) studied the anodic behaviour of Co, W, and WC in nitrate and chloride solutions. Common commercial electrolytes such as $NaNO_3$ (250 g L21) or sodium chloride were employed at the foundation (125 g L21). Various methodologies were used to calculate the current reliance on products: (i) via fluorescence extinction of the dichlorotris ruthenium, the hydrate and oxygen were specifically out; (ii) cobalt was measured through colourimetric measurement; and (iii) tungsten was determined colourimetrically using Alizarin Red S. Inside $NaNO_3$ and sodium chloride solutions, W is not melted, and pure WC is not liquified. Cobalt dissolution processes WC/Co; WC particles are quickly swept away, leading to poor surface superiority. As a result, electrolyte adjustments are required. Rataj et al. concentrated on the WC6Co ECM (Wang et al., 2022). WC6Co specimens were processed through grinding by SiC leaf of various polishing degrees to a shiny surface through a diamond postponement. To avoid a chemical assault on the complex or binder phase, the planning was completed without using chemical etching or

Figure 4
Cobalt and electropolished tungsten wires at low potentials show cyclovoltammograms in an aqueous $NaNO_3$ solution

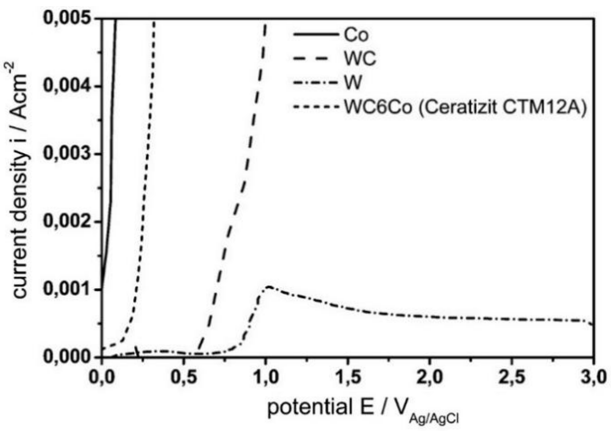

Figure 5
Cobalt and electropolished tungsten wires in aqueous $NaNO_3$: Cyclovoltammograms at low potentials revealing WC/Co examples

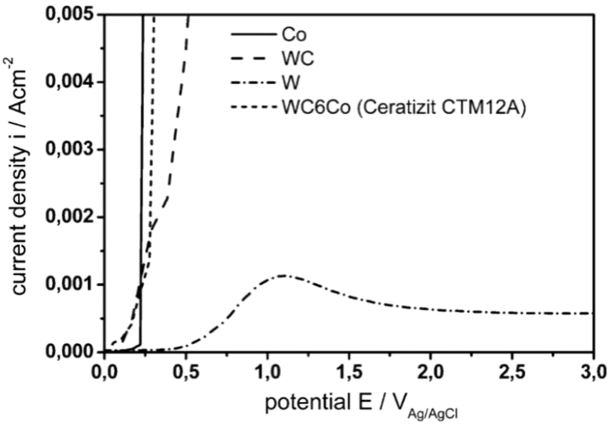

polishing techniques. Figures 4 and 5 (Lohrengel et al., 2014) depict cyclovoltammograms of cobalt and electropolished tungsten wires, pure WC, then saleable WC/Co examples in the aqueous solution of $NaNO_3$, and Figure 6 (Lohrengel et al., 2014) is about investigations on the current transients of a 5 s potentiostat, pure WC in aqueous sodium chloride. Figure 7 (Lohrengel et al., 2014) depicts the microstructure. The grains of WC are soft grey. WC grain breaches

Figure 6
Investigations on the current transients of a 5 s potentiostat, pure WC in aqueous sodium chloride

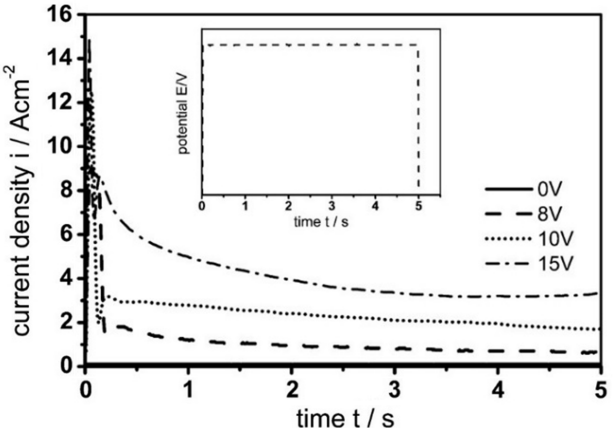

are incorporated in the cobalt binder substance (dark areas). The average size of the WC units is about 1.5 µm.

The complex and binder phases of tungsten carbide–cobalt (WC–Co) are superimposed (Hochstrasser-Kurz, 2006; Kellner et al., 2009). The dissolution of WC subjugates the WC–Co electrochemical performance in an alkaline-type solution with potentials $0 \geq$ V(SHE). The diagram of Pourbaix suggests that the response crops in an alkaline-type solution at 25uC are carbonate and tungstate. WC–Co corrosion tests have revealed that WC dissolves in a two-phase process (Andersson & Bergström, 2000; Hochstrasser-Kurz, 2006). The first phase is an oxidation response exposed in equation (2), followed by a chemical process exposed

Figure 7
Ceratizit microstructure as seen using a scanning electron microscope

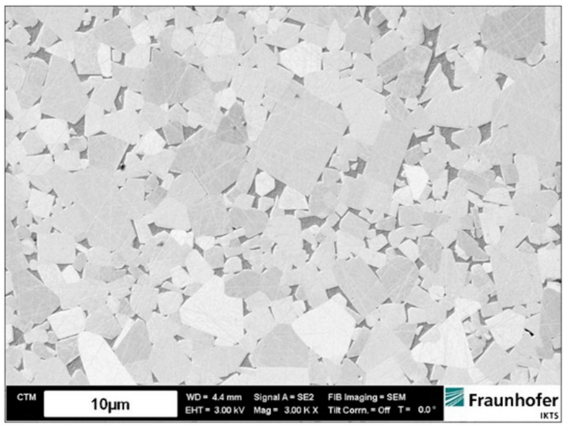

in equation (3). As exposed in equation (4), the entire response for WC disbanding in the given electrolyte is supposed.

$$\mathrm{WC} + 6\mathrm{H_2O} \rightarrow \mathrm{WO_3} + \mathrm{CO_3^{2-}} + 12\mathrm{H^+} + 10e^- \quad (2)$$

$$\mathrm{WO_3} + \mathrm{H_2O} \rightarrow \mathrm{WO_4^{2-}} + 2\mathrm{H^+} \quad (3)$$

$$WC + 7H_2O \rightarrow \mathrm{WO_4^{2-}} + \mathrm{CO_3^{2-}} + 14\mathrm{H^+} + 10e^-, \quad E^0 = 0.176V_{\mathrm{SHE}} - 0.0807VpH \quad (4)$$

Based on thermodynamic considerations, the authors assume the Co binder phase passivation in an alkaline-type solution (Pourbaix, 1974). Different oxides or hydrides can create (Göhr, 1966; Schubert et al., 2013), as illustrated in equations (5)–(9).

$$Co + 3\mathrm{H_2}O \rightarrow CoO + 2\mathrm{H_3O^+} + 2e^-, \quad E^0 = 0.095V_{\mathrm{SHE}} - 0.0591VpH \quad (5)$$

$$Co + 4\mathrm{H_2}O \rightarrow Co(OH)_2 + 2\mathrm{H_3O^+} + 2e^-, \quad E^0 = 0.166V_{\mathrm{SHE}} - 0,0591VpH \quad (6)$$

$$3CoO + 3\mathrm{H_2}O \rightarrow \mathrm{Co_3O_4} + 2\mathrm{H_3O^+} + 2e^-, \quad E^0 = 0.993V_{\mathrm{SHE}} - 0.0591VpH \quad (7)$$

$$3Co(OH)_2 \rightarrow \mathrm{Co_3O_4} + 2\mathrm{H_3O^+} + 2e^-, \quad E^0 = 0.777V_{\mathrm{SHE}} - 0.0591VpH \quad (8)$$

$$\mathrm{Co_3O_4} + 6\mathrm{H_2}O \rightarrow 3Co(OH)_3 + \mathrm{H_3O^+} + e^-, \quad E^0 = 1.018V_{\mathrm{SHE}} - 0.0591VpH \quad (9)$$

Oxygen growth is a secondary effect with potentials larger than 0.42 V(SHE) (Pourbaix, 1974). WC dissolution and oxygen evolution may occur concurrently during the binder phase.

Shibuya et al. (2012) suggested and examined the machining conditions for micro-pins manufactured of WC alloy by the ECM with an aqueous neutral $NaNO_3$. The micro-pins were created by adjusting electrolyte content, current value, and machining time. With a steady current of 400 mA, the diameter of the micro-pin was around 20 µm, the length was around 2 mm, and the aspect proportion was around 100. It was created in 2.5 min. Figures 8, 9, and 10 (Shibuya et al., 2012) provide further information. Due to the intense concentration of electrolyte stopping the current from concentrating at the pin's end, the electrolyte concluded a convincing awareness. For instance, a 1% concentration, less than the conditions of this test, is

Figure 8
The connection between voltage and machining time at various emphases

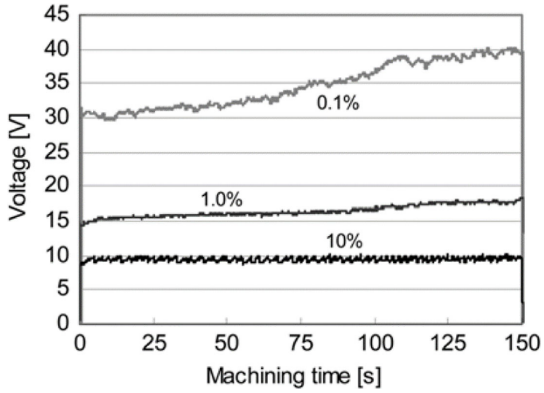

Figure 9
Under 10% concentrations, the detailed connection between machining time and voltage is shown

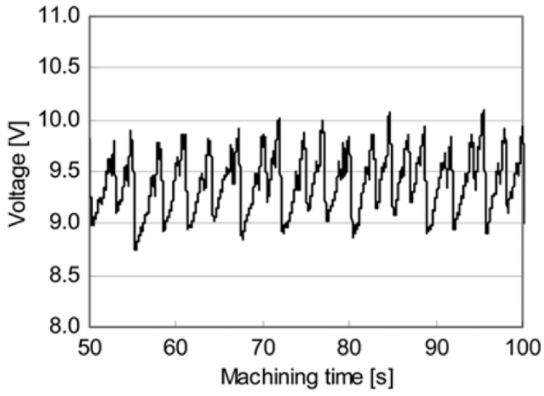

required for acquiring micro-pins by an unvarying diameter. Minor machining currents are advantageous to producing micro-pins with a narrower taper angle. The time of machining may be used to adjust a pin diameter.

5.2. The mixture of ammonia and sodium nitrate

Schubert et al. (2014) investigated the WC–Co behaviour in alkaline ammonia electrolytes at near-ECM conditions. The

Figure 10
The connection between pin diameter and machining time at various streams

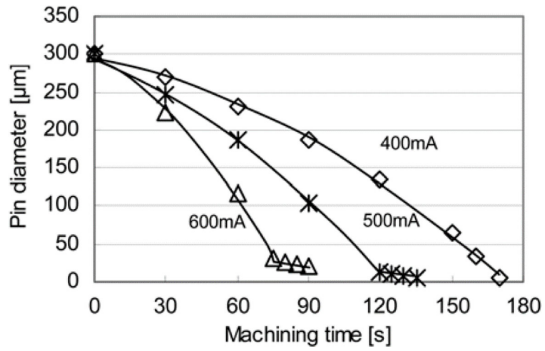

electrolyte was a $NaNO_3$ and ammonia mixture (as shown in Table 3 (Schubert et al., 2014)). The material utilised was readily accessible on the market. Ceratizit samples (Ceratizit, n.d) of CTM12a ($WCCo_6$) were equipped by grinding via SiC paper (up to P1200) and polishing with di-suspension to a mirror-like surface. Measurements for reference were collected on pure cobalt and pure WC. A cell with a microcapillary flow path was used for experiments. Figure 11 (Schubert et al., 2014) shows a schematic picture of the capillary crystal tip on the left side and a snapshot of the entire cell on the right side. It permits investigations utilising conventional potentiostats and laboratory circumstances under near-ECM conditions (Lohrengel & Rosenkranz, 2005; Schubert et al., 2013).

Table 3
Classification of the electrolytes utilised

Electrolyte	Concentration	pH value	Conductivity
$NH_3/NaNO_3$	2.0/2.9 (mol L^{-1})	12	151 (mS cm^{-1})

This combination achieves standardised dissolving of both the complex and binder phases. Although cobalt dissolves quietly, WC dissolves vigorously. At 5 A cm^2, the current efficiency is near 100% but drops to around 70% for 20 A cm^2 and greater current densities. Energy-Dispersive X-Ray Spectroscopy (EDX) and scanning electron microscope (SEM) investigations back up this claim. The results are depicted in Figures 12, 13, and 14 (Schubert et al., 2014).

Figure 11
WE: anode, CE: cathode, microcapillary flow over the cell, and a graphically expanded crystal capillary tip

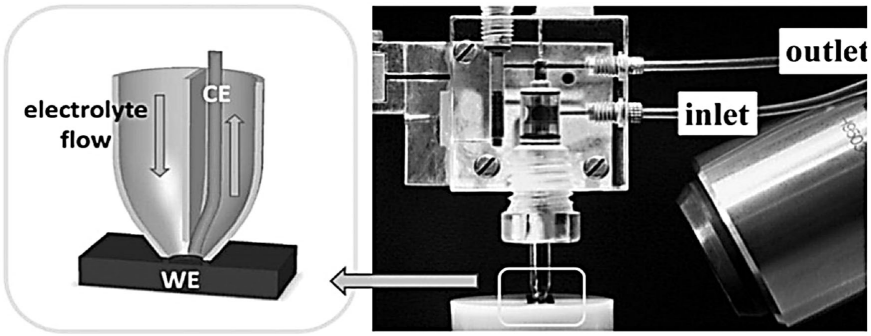

Figure 12
Cyclic voltammograms, dE/dt, is 50 mV/s, E = −0.90–1.00 V, $NH_3/NaNO_3$ (2.0 M/ 2.9 M), grey dashed line: Co (dE/dt is 0.5 V/s)

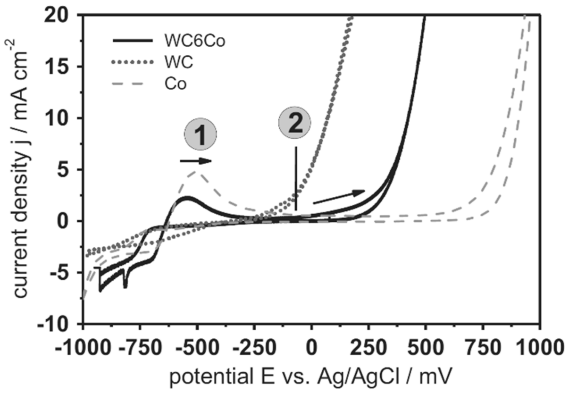

Figure 14
Concerning current density, the current efficiency of WCCo6 ECM with $NH_3/NaNO_3$

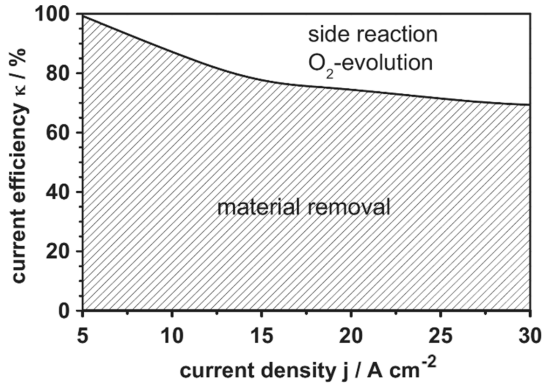

5.3. Hydroxide of sodium

Schubert et al. (2018) tested commercial tungsten with a purity of 99.95% and non-commercial, binder-free WC samples. These binder-free samples were made in-house (IKTS) by sintering two WC powders with similar chemical compositions but differing particle sizes. Characteristics of the WC powder utilised are available in Table 4 (Schubert et al., 2018). Figure 15 (Schubert et al., 2018) shows SEM pictures of WC samples. The tungsten

Table 4
Characteristics of the WC powder utilised. The d indices denote the proportion of powder particles of the specified sizes

Powder	d_{90} (/µm)	d_{50} (/µm)	d_{10} (/µm)	*C* (%)	*O* (%)
WC600	20.9	10.1	4.2	6.09	0.03
WC2000	121.9	42.6	15.9	6.15	0.01

Figure 13
SEM WCCo6 (CTM12a) pre-ECM; (a) WC hard bright; co binder shaded. (b) Mark 1 Co binder, mark 2 WC hard, machined in $NH_3/NaNO_3$. (c) The post-machining EDX of the binder. (d) Post-machining complex phase EDX observation

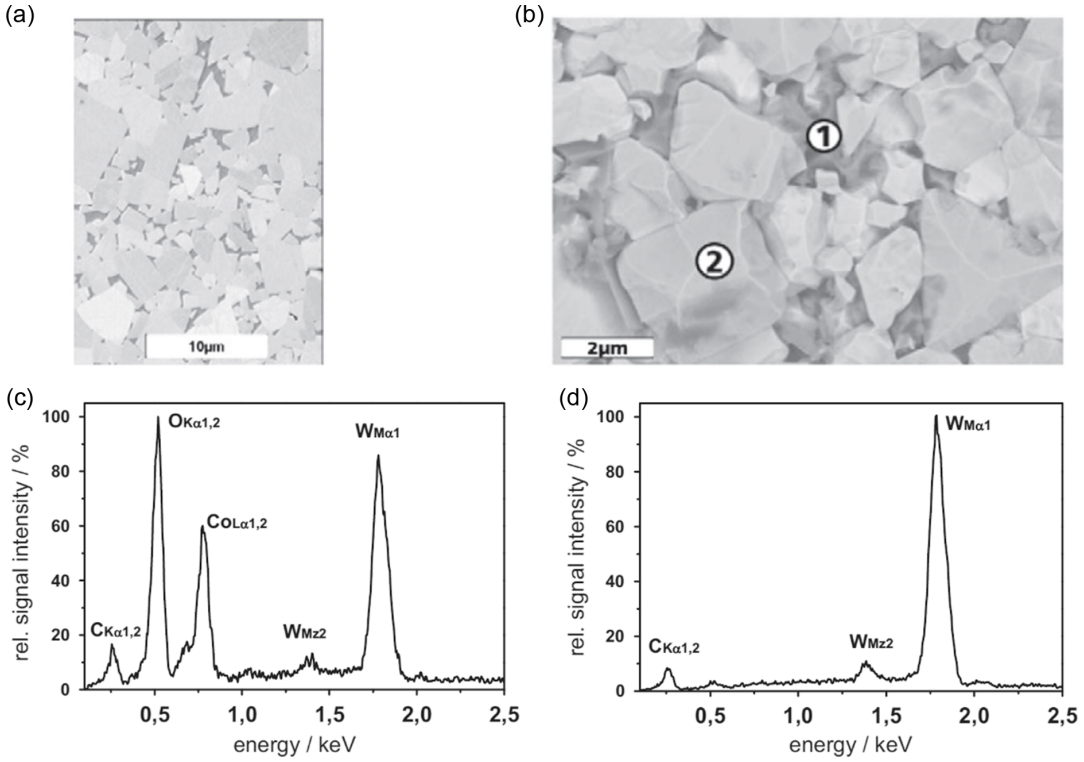

Figure 15
Left WC600, right WC2000, SEM pictures of WC samples (magnitude 1000)

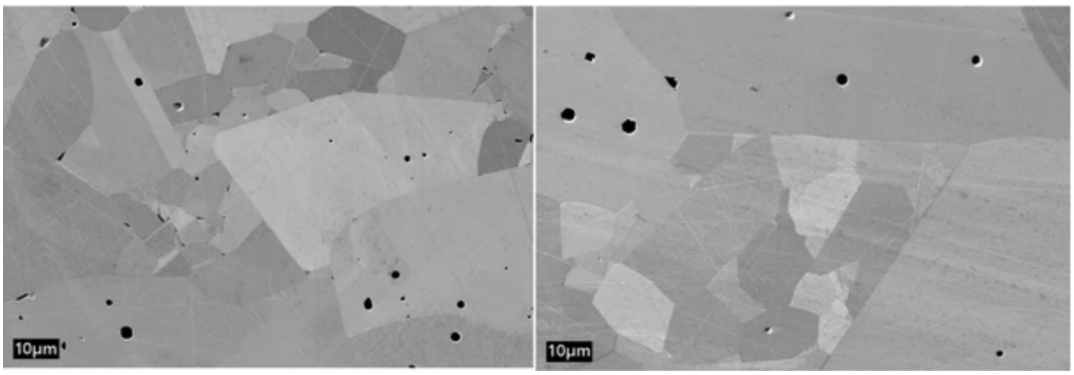

sample was mechanically ground with SiC paper before polishing with diamond suspensions of varying grain sizes (15, 3, 1, 0.1 µm). The WC tasters were mechanically slurped. The samples were cleaned with deionised water and degreased with ethanol before testing. The electrolyte was a 1 M NaOH solution comprised of sodium hydroxide pellets p.a. (Carl Roth) and deionised water.

Highly stable oxide layers protect tungsten in air and neutral and acidic fluids (Aladjem et al., 1970). As a result, in combination with equation (10), the oxide is generated in acidic or neutral solutions. The oxide is classified as amorphous WO_3.

$$W + 3H_2O \rightarrow WO_3 + 6H^+ + 6e^- \quad (10)$$

Acidic medium corrosion produces "tungstenyl" cations.

$$W + 2H_2O \rightarrow WO_2^{2+} + 4H^+ + 6e^- \quad (11)$$

Alkaline solutions are where tungstates are formally produced.

$$W + 4H_2O \rightarrow WO_4^{2-} + 8H^+ + 6e^- \quad (12)$$

Furthermore, condensation processes can polymerise into polytungstates, such as:

$$W + 4H_2O \rightarrow WO_4^{2-} + 8H^+ + 6e^- \quad (13)$$

When the field strength is more than 6 MVcm1, the anodic oxide layer grows through a high-field mechanism (Ammar & Salim, 1972; Ammar & Salim, 1971; Arora & Kelly, 1977; Quarto et al., 1980). At 100 µAcm−2, the transported cations are 0.35, increasing somewhat with current density (Khalil & Leach, 1986). In aqueous NaCl, $NaNO_3$, and H_2SO_4, they discovered tiny peaks in activation about 1 V (Schubert et al., 2018), then a steady plateau stream follows, iPlateau, of 190 µA.cm^2 at the rate of a sweep of 100 mV/s (Rataj, 2013). The cathodic sweep currents are almost negligible, consistent with valve metals' typical behaviour and high-field advancement (Schubert et al., 2018).

WC behaves in a manner that is identical to that of W. Equation (14) shall be followed for anodic WC dissolution in alkaline solutions:

$$WC + 7H_2O \rightarrow WO_4^{\ 2-} + CO_3^{\ 2-} + 14H^+ + 10e^- \quad (14)$$

Thermodynamic results must not match ECM systems with 10 or 100 A cm^{-2} current densities, a long way from electrochemical balance. The hydrodynamic edge layer permits the creation of a thin layer of reaction products that are strongly supersaturated, which exists despite the high electrolyte velocity. Protons are released in large quantities, which causes a significant pH change to lower levels. According to typical diffusion models, buffering the surface of the metal with NaOH (1 M) will be effective in reaching densities of around one A cm^2, but not under ECM conditions (Schubert et al., 2018)

6. CM Operations and Modes

6.1. Jet-ECM

The anodic sample and the cathodic tool in Jet-ECM are connected in a straight electric current (Hackert-Oschätzchen et al., 2012), as illustrated in Figure 16 (Hackert-Oschätzchen, et al., 2013c). A simple nozzle drives the electrolytic, expelled at an average speed of around 20 m.s^{-1}. The cast-out liquid forms a closed-free jet due to the lack of mixing with the atmospheric air-based environment, which has a substantially lower density (Truckenbrodt, 1996). Because the electrolyte flows steadily, the jet has a well-defined geometric form. An endless supply of electrolytes with consistent pressure is guaranteed by utilising a pulsation-free pump.

Jet-ECM methods use continuous, direct current, which results in faster-dissolving rates than pulsed EC techniques. Because of the high jet rate, this is made possible by an excellent source of fresh electrolytes. There is no longer any need to halt the operation for flushing stages. For all of these benefits, Jet-ECM has tremendous potential for shaping carbide metals. Natsu et al. examined using Jet-ECM to quickly machine complicated three-dimensional structures in metallic WPs (Natsu et al., 2008; Natsu et al., 2007). Compound

Figure 16
Schematic of Jet-ECM

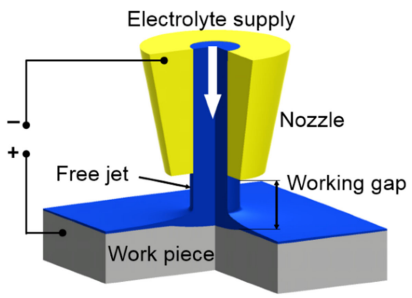

micro geometries may be formed with this technique by controlling the nozzle and electric current motion (Hackert et al., 2010). No need will arise to create complex electrode configurations in the future, as in electrochemical plummeting applications. Schubert and colleagues examined suitable electrolytic materials for cobalt machining, cemented carbides' the most crucial metallic binder (Schubert et al., 2011). As a result, alkaline solutions were employed, which ought to be appropriate for WC machining. Numerous investigations have been conducted on the dissolving behaviour of cemented carbides, focusing on two-dimensional shaping (Bozzini et al., 2003; Masuzawa & Kimura, 1991; Walther et al., 2007). Figure 17 (Hackert-Oschätzchen, et al., 2013c) depicts a diagram of the prototype system, its fundamental parts, and their relations. The electrolyte scheme comprises a filter unit, a pulsation-free drive, and tubes with high pressure. The electrolytic is therefore expelled in the Z-direction while being linked to the nozzle. In a dumping tank, the used electrolyte is collected. The generator system generates electricity. A three-axis positioning apparatus was devised to be aware of the nozzle's and the WP's relative movement. Figure 18 (Hackert-Oschätzchen, et al., 2013c) is a shot of this prototype facility's procedure chamber.

Figure 17
Jet-ECM prototype system schematic drawing

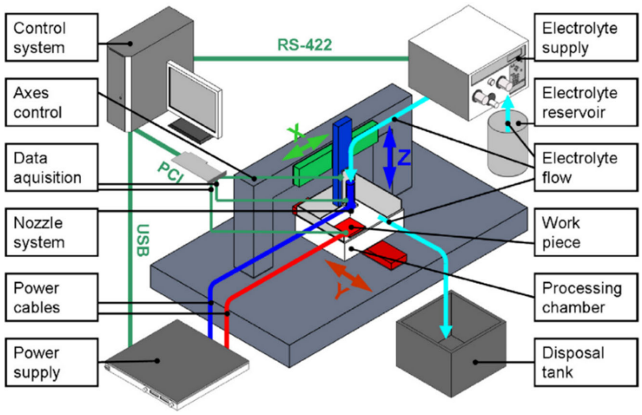

Figure 18
Jet-ECM process chamber photo

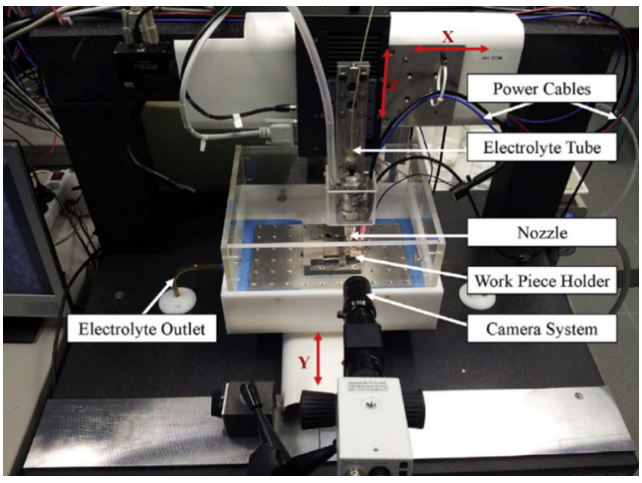

Figure 19
A depth graph of the Jet-ECM fabricated object and a drawing of geometrical measures was taken

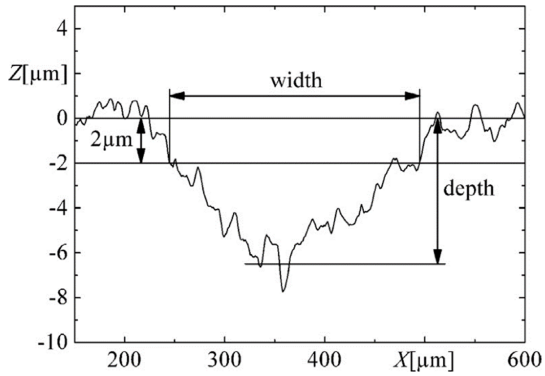

Hackert-Oschätzchen, et al. (2013c), in an investigation, suggested Jet-ECM as a viable approach for cutting alloys of WC. Several machining tests were carried out using a Jet-ECM prototype facility. Erosion of points was performed at cumulative processing durations; then, grooves were carved to investigate the effect of nozzle speediness. In addition, the increased gap voltage and growing electrolytic conductivity were evaluated. Figure 19 (Hackert-Oschätzchen, et al., 2013c) depicts the geometric measurements and the cross-sectional profile of a Jet-EC machined groove.

By layering linear erosions with cumulative crossing numbers and varying nozzle speediness, the capability of machining three-dimensional structures without a formed electrode was established. Plane surfaces were possible with minimal reserves between the erosions, but broader aloofness produced kinematic roughness.

6.2. ECM surface finishing

A customised pulse train design for varied separation ECM is planned to comprehend uniform WC dissolution and overpower the tool electrode's dissolving. Masuzawa and Kimura (1991) conducted an experimental investigation on the surface finishing of WC alloy. By applying the pulse to an EDMed surface, the efficiency was determined. A flat surface was created with no heat-affected layer or fissures. The trials also yielded suggestions for choosing an electrode material. Figures 20 and 21 (Masuzawa & Kimura, 1991) are related to this experiment.

6.3. Electrochemical etching

Muller and Tsong (1969) used electrochemical etching to create a tungsten micro-probe aimed at Field ion microscopy (FIM). Many investigators have explored micro-tip fabrication for Scanning tunneling microscope (STM) and Atomic force microscope (AFM). Choi et al. (2006) performed an electrochemical etching experiment on the micro-shaft of WC. A diagram of the utilised system is shown in Figure 22 (Choi et al., 2006). H_2SO_4 was the electrolyte which instantly dissolved cobalt and tungsten. The optimal electrolyte content and voltage used were chosen empirically to produce a WP with an unvarying form, decent surface quality, and significant MRR. Controlling the different machining constraints resulted in an orthodox micro-shaft with a 5 µm diameter and a 3 mm length. They machined a high-quality micro-hole with an 8 µm diameter and a micro-groove with a 9 µm width in stainless steel 304, utilising produced micro-shafts

Figure 20
Electrode wear is caused by different electrode materials

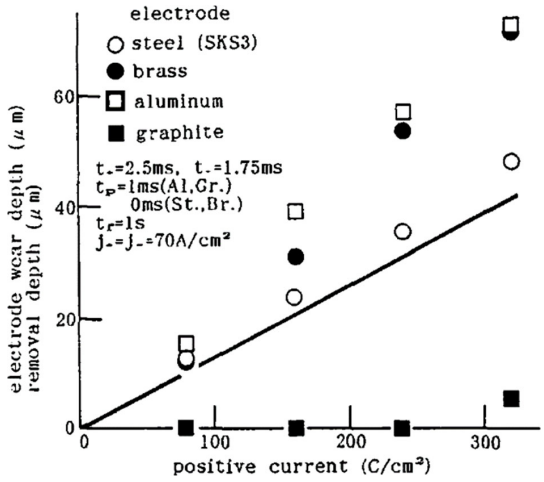

Figure 21
Improvement of roughness using graphite electrode

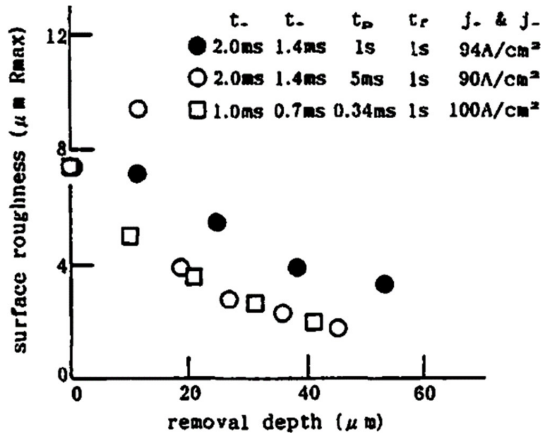

Figure 22
Electrochemical etching system schematic diagram

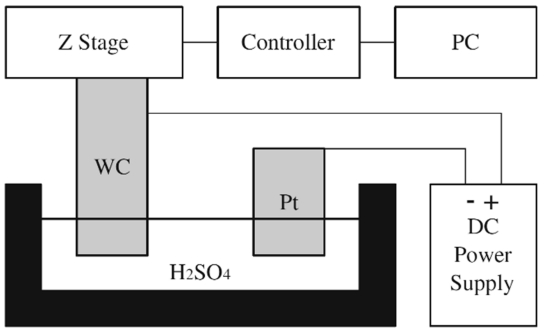

Figure 23
Sludge accumulation on the sample during the etching of WC

Figure 24
Measure the workpiece's diameter following the electrolyte concentration at 210 seconds of machining time and voltage of 4.1 V

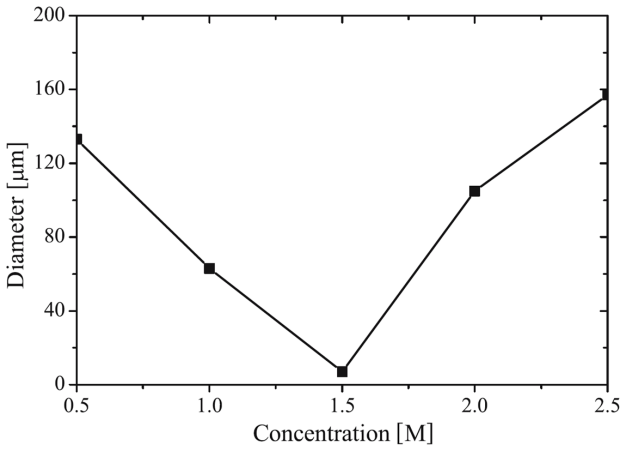

Figure 25
Workpiece diameter at applied voltage, 1.5 M H_2SO_4 as the electrolyte, and 210 s of machining

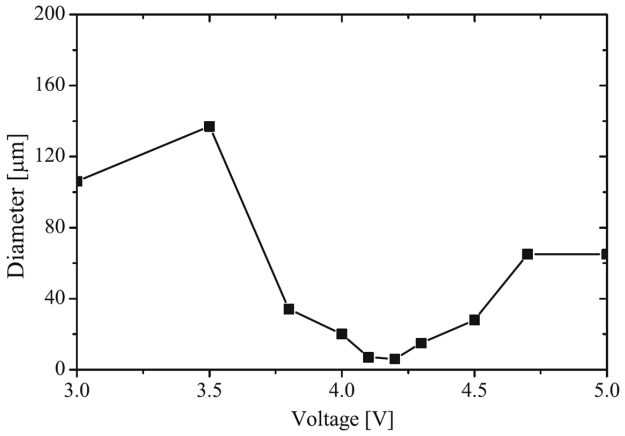

Figure 26
The workpiece's diameter is determined by the time spent cutting it with electrolyte 1.5 M H_2SO_4 and 4.1 V of applied voltage

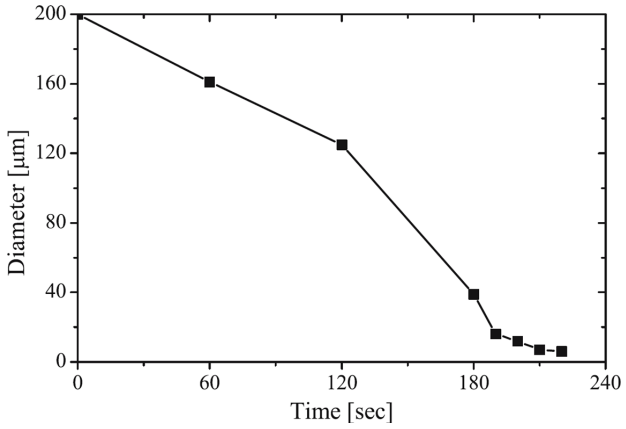

Figure 27
Desktop micro-ECM system illustrated schematically

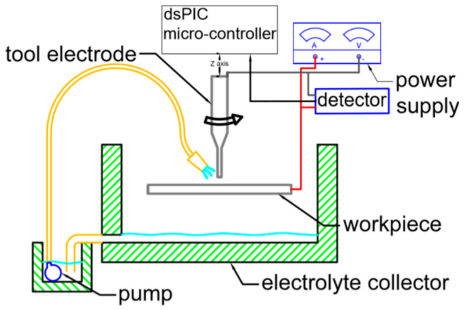

for use as tools (304 SS). Some critical points of this experiment are presented in Figures 23, 24, 25, and 26 (Choi et al., 2006).

The electrolyte for the manufacture of micro-shafts was WC with a Co binder. With a voltage of 4.1 V, a 1.5M H_2SO_4 solution, and 210 seconds of machining, a 5 µm diameter and 3 mm length were produced. By immersing the shaft in a NaOH solution, the sludge that had accumulated on the sample was released. On 304 SS, small micro-holes and a micro-groove were carved using a few tens of nanosecond pulses and localised electrochemical dissolution. That is what is anticipated; this method may be used to create a variety of three-dimensional microstructures.

6.4. Micro-ECM

For applications requiring micro-nozzles, WC–Co offers the necessary hardness and reduced wear. The most widely used techniques for processing WC–Co materials are grinding, Laser beam machining (LBM), Electron beam machining (EBM), EDM, and ECM (Rajurkar et al., 1999). Conventional grinding can also produce an excellent WP surface, but producing products with intricate shapes is still challenging, and its MRR is poor. Micro-ECM and micro-EDM are often utilised for drilling minute holes into WC–Co WPs (Mithu et al., 2011; Sundaram & Rajurkar, 2010). Wu and Sheu (2018) established a low-cost desktop micro-ECM for studying the properties of micro-hole drilling of WC. The presentation characteristics of the desktop micro-ECM machining settings, including material removal rate, the machining time, surface quality, relative tool wear rate, and dimensional accuracy, were examined by that research.

Figure 27 (Wu & Sheu, 2018) depicts a desktop micro-ECM schematic, its essential parts, and their relations. The desktop micro-ECM contains an X axis, a Y axis, and a Z axis for drilling micro holes. The micrometre screw gauge is used to find the X-Y direction manually, and the microcontroller unit may regulate the Z-axis. The block with a V-shape is the most significant feature of the desktop micro-ECM because it maintains focus and uncurls tools for the spindle electrode. The spindle tools are held in place by a V-shaped block and controlled via the motor. The spindle tools and electrolyte flow are contained in the electrolyte collector. The spinning speed may be adjusted. The linear straightness and roundness of micro-hole drilling are critical for achieving high precision. Figures 28 and 29 (Wu & Sheu, 2018) depict the whole structure of this desktop micro-ECM.

Micro-ECM machining produces smoother surfaces with lower wear rates and friction coefficients than EDM. The electrochemical dissolution micro-ECM machining can completely detach WC–Co,

Figure 28
Structure of desktop micro-ECM

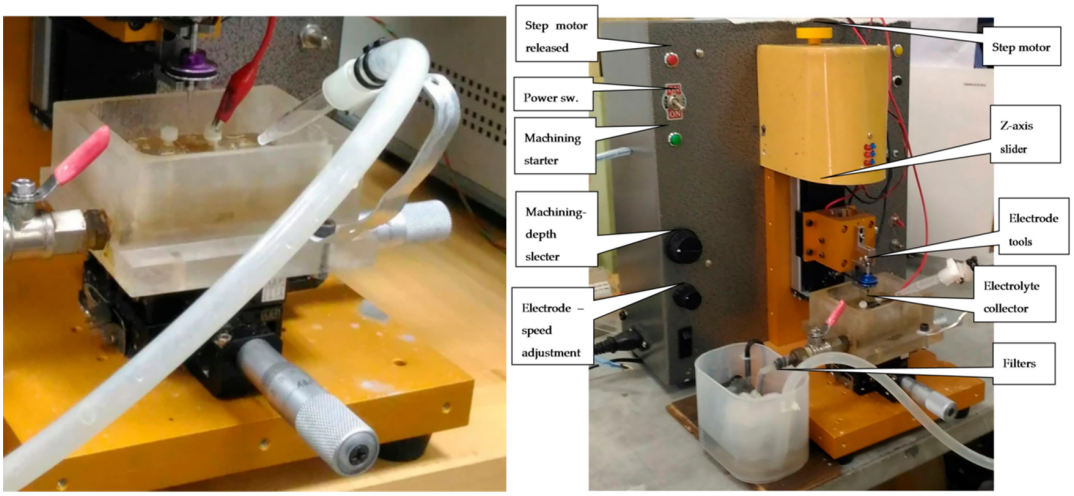

Figure 29
With the aid of a pulley, the spindle micro-tool revolves on the V-shaped block. Spindle electrode tool to start. (b) A pulley-equipped spindle micro-tool. (c) The V-shaped block spins around the microtool

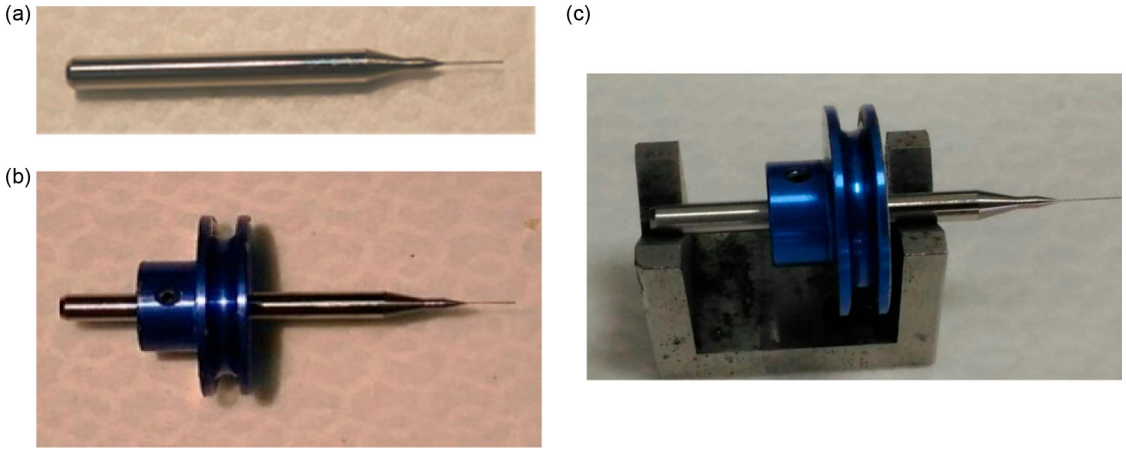

Table 5
Information on the desktop micro-ECM's feeding depth

	Time (min)							
Current	40	30	25	20	15	10	5	0
0.5(A)	455	260	210	160	110	80	30	0
1(A)		455	350	245	180	145	60	0
2(A)			455	370	300	200	150	0
3(A)							170	0

Table 6
Data on updates to micro-tools

	Voltage (V)			
Tool (μm)	20 V	10 V	15 V	5 V
After machining	3647	3615	3637	3620
Before machining	3632	3620	3615	3645
Tool change	15	− 5	12	− 25

and the established desktop micro-ECM can carry out WC–Co micro-hole drilling. According to Wu and Sheu (2018), it employed the micro-ECM and made precise micro-holes in WC–Co materials. This study sets the electrolytic current and working voltage to optimal levels of 10 V and 3 A. The experimental findings demonstrated that proper machining limitations, excellent machining efficiency, and acceptable surface quality are feasible for practical applications. Tables 5 and 6 and Figure 30 (Wu & Sheu, 2018) are about this research.

6.5. Electrochemical wire grinding

The demand for micro-rods and probes for measurement systems is rising due to the widespread usage of micro-rods as tools for micro-drilling and micro-milling 3D constructions (Masuzawa, 2000). ECM is advantageous for machining micro-rods because it is an anodic dissolution process (Rajurkar et al., 1999) devoid of residual tension and surface fractures that are invariably produced in thermal processes like EDM and laser machining. Tungsten is commonly utilised as a micro-rod material because of its strong erosion resistance, high electrical and thermal conductivity, and substantial stiffness. However, ECM of tungsten is challenging. Lim and Kim (2001) and Fan and Hourng (2009) employed KOH and NaOH aqueous solutions as electrolytes for creating tungsten rods. Nevertheless, neutral electrolytes must be used instead because alkaline-based electrolytes are incredibly damaging to the ecology. According to Maeda et al. (1967), it is possible to machine cemented WC using a bipolar current and a neutral electrolyte, such as an aqueous solution of $NaNO_3$, because while the WC electrode is in the negative polarity, it creates NaOH, eliminating the oxide layer from the surface of the WC. Thus, Natsu and Kurahata (2013) successfully machined cemented WC rods via an aqueous solution of $NaNO_3$. However, the accuracy was insufficient to create micro-rods comparable to those achieved by the EDM method. There was dramatically increased wear on the tool from the current that is bipolar. Schuster et al. (2000) propose that the ECM method can be implemented once an ultra-short pulse current with a time of many tens of nanoseconds is utilised. The electrostatic induction feeding ECM was manufactured by Koyano & Kunieda, (2013). Figures 31 and 32 (Koyano & Kunieda, 2013) depict the method's equivalent circuit, voltage waveforms, and gap current. A pulse voltage is applied across the work gap, and the electrodes' surface develops an electric two-fold layer, which C_{dl} denotes. As a result, the working gap may be established as the Faraday impedance R_f, electrolyte resistance in the machining gap R_g, and C_{dl} (Bard & Faulkner, 1980).

Next, using a bipolar current and neutral electrolyte such as NaCl or $NaNO_3$ aqueous solution, Han & Kunieda (2017) created tungsten micro-rods. They successfully created a micro-rod (diameter = 7.1 μm and aspect ratio = 14) employing an ultra-short pulse current of 20–40 ns to localise electrochemical dissolution in a narrow working gap. For the first time, Masuzawa et al. (1985) employed a micro-EDM wire tool electrode to create micro-rods without being affected by tool wear brought on by discharge, a process known as wire electro-discharge grinding (WEDG). To avoid the wire vibration that often occurs in wire EDM, a cylindrical leader with circumferential flutes is used in WEDG to support the wire. Researchers could electrochemically grind tungsten micro-rods with remarkable precision using the same tool electrode configuration for electrochemical wire grinding and a bipolar current (Han & Kunieda, 2018). Figure 33 (Han & Kunieda, 2018) depicts the wire electrochemical grinding (WECG) approach. By swapping out the

Figure 30
Compared to micro-ECM machining, micro-electrical discharge machining (EDM) (a) EDM's surface is more consistent, like the grapefruit peel. (b) The ECM's surface was even and smooth

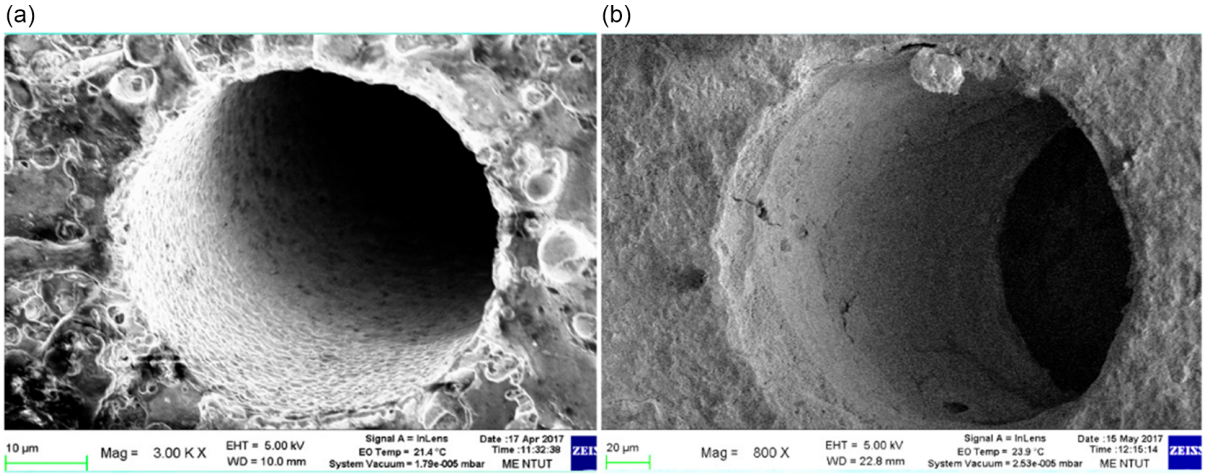

Figure 31
ECM fed via electrostatic induction

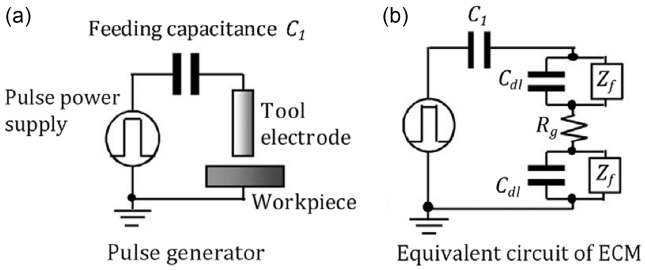

Figure 33
Method of wire electrochemical grinding

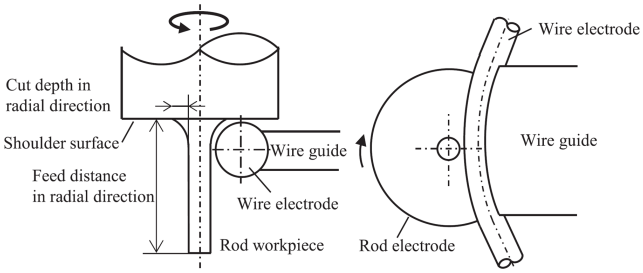

Figure 32
Electrostatic inductive feeding ECM theory

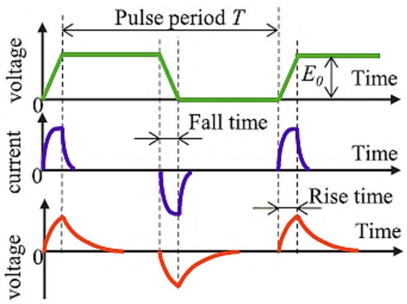

circuit for the EDM pulse generator shown in Figure 31 (Koyano & Kunieda, 2013), the micro-electrical discharge machine (MG_ED72W, Panasonic) converted into a micro-ECM. The diameter commercial brass wire of 100 µm, held by the wire director, serves as a tool electrode and is kept in a row while machining. When using a wire tool electrode throughout the machining procedure, it is possible to ignore how the bipolar current's impact on tool wear will affect the accuracy of the operation.

WECG was featured in research by Han and Kunieda (2018) to produce tungsten micro-rods using the electrostatic induction feeding technique, neutral electrolyte aqueous solution of $NaNO_3$, and bipolar current. Some significant inferences were reached. First, the successful machining of tungsten micro-rods was achieved using the suggested process of WECG. Once the operating speediness of the tool electrode was 53.3 mm min^{-1}, the influence of bipolar current on tool wear was noticeably modest. Additionally, three types of wire guides' machining properties were considered when the WP was fed axially: WC guide cylindrical cemented, ZrO_2 cylindrical guide, and cemented WC guide in the shape of a disk. The best machining was on the WC wire guide in the form of a disk. Micro-rods, on the other hand, were successfully machined when the WP was supplied radially. The current efficiency was reduced contrasted with the WP supplied approach in an axial fashion. Finally, using an axial feed WP, micro-rods with a 100 µm span can manufacture to a length of 850 µm in one machining stage. Smaller-sized rods of 35 µm and 163 µm micro-rod lengths were produced after two machining processes, demonstrating micromachining capacity equivalent to micro-EDM (Han & Kunieda, 2018).

7. Conclusion

ECM is a non-traditional process with many benefits over conventional machining methods, such as its independence from the material's mechanical properties, the absence of outstanding surface integrity, tool wear, low machining cost, and high

machining efficiency. In the aerospace, medical, and automotive industries, precise machining complicated forms and difficult-to-machine materials are efficient techniques. The technique is mainly used to assess the conductivity of conductive materials, such as metals with rough surfaces. The material is separated from the WP due to the anodic dissolution of the WP material in water-based electrolytes at extraordinary current densities.

Articles with the keywords "electrochemical machining" or "ECM" and "tungsten carbide" or "WC" were included in the database of reviewed articles. The primary focus of this review article was on the electrochemical properties of WC and its application in ECM. It was discussed how WC behaves anodically as it applies to ECM, which experiments were conducted with various electrolytes, and how they performed. Several ECM mods have been considered, and each mod has been evaluated in detail for challenges and gaps. The following results were obtained.

- Electrolytes must be modified to obtain successful machining of pure WC.
- In alkaline conditions, nitrates and hydroxides generate supersaturated product coatings with a polishing action, allowing ECM to be effective.
- $NaNO_3$ aqueous solution, rotation, and ultrasonic cleaning can create WC alloy micro-pins.
- In order to create micro-pins with a consistent diameter and prevent current from condensing at the pin's end, a highly concentrated electrolyte is required.
- Cemented carbide's electrochemical behaviour ($WCCo_6$) is a cobalt–tungsten carbide phase superposition.
- The electrolyte combination of $NaNO_3$ and ammonia produces homogeneous dissolution of $WCCo_6$ under ECM conditions.
- Jet-ECM is a possible micro-manufacturing process that allows the machining metallic WP components without mechanical or thermal impacts. It is a viable alternative to traditional procedures and offers a high degree of versatility and a wide range of options for machining surfaces and micro geometries.
- Jet-ECM is a prospective technology for WC alloy machining: more significant salt fraction, extended processing periods, and gap voltages result in more profound and narrower structures.
- Controlling the electric current in Jet-ECM is ideal for eliminating WC alloys because it raises the optimal voltage and lowers process resistance. Deeper developing structures raise the voltage optimum, increasing process resistance.
- The electrostatic induction feeding approach produced a micro-ECM system with ultra-short pulses. It was created as a servo feed control system. Micromachining with narrow gap widths was shown by lowering pulse length and voltage while increasing feed speed.
- Utilising bipolar current and neutral electrolyte, a WECG process effectively machined tungsten micro-rods while minimising tool wear by 53.3 mm/min. The disc-shaped WC wire guide demonstrated the finest machining accuracy, allowing the machining of micro-rods (diameter = 100 μm) in one step to a length of 850 μm.

In conclusion, the ECM of WC and its alloys face some problems and challenges. However, modifying the electrolytes and optimising the technological equipment and process of ECM of WC are beneficial to improving the machining accuracy and stability.

Conflicts of Interest

Mohammed Asmael is the Associate Editor for *Archives of Advanced Engineering Science*, and was not involved in the editorial review or the decision to publish this article. The authors declare that they have no conflicts of interest to this work.

Data Availability Statement

Data sharing is not applicable to this article as no new data were created or analyzed in this study.

References

Aladjem, A., Brandon, D. G., Yahalom, J., & Zahavi, J. (1970). Electron-beam crystallization of anodic oxide films. *Electrochimica Acta*, *15*(5), 663–666. https://doi.org/10.1016/0013-4686(70)90029-0.

Alla Chaitanya, C. R., Wang, N., & Takahata, K. (2010). MEMs-based micro-electro-discharge machining (M3EDM) by electrostatic actuation of machining electrodes on the workpiece. *Journal of Microelectromechanical Systems*, *19*(3), 690–699. https://doi.org/10.1109/JMEMS.2010.2047845.

Ammar, I. A, & Salim, R. (1971). Anodic behaviour of tungsten-I. Oxidation kinetics in acid media. *Corrosion Science*, *11*(8), 591–609. https://doi.org/10.1016/S0010-938X(71)80056-2.

Ammar, I. A., & Salim, R. (1972). Anodic polarization of tungsten in neutral and alkaline solutions under conditions of anode film growth. *Werkstoffe Und Korrosion*, *23*(3), 161–167.

Andersson, K. M., & Bergström, L. (2000). Oxidation and dissolution of tungsten carbide powder in water. *International Journal of Refractory Metals and Hard Materials*, *18*(2-3), 121–129. https://doi.org/10.1016/S0263-4368(00)00010-X.

Arab, J., & Dixit, P. (2020). Influence of tool electrode feed rate in the electrochemical discharge drilling of a glass substrate. *Materials and Manufacturing Processes*, *35*(15), 1749–1760. https://doi.org/10.1080/10426914.2020.1784936.

Arafat, M., & Fanghua (2020). A Review on recent studies: Non-traditional machining of titanium alloys. *EngrXiv preprint:* https://doi.org/10.31224/osf.io/sf2xg.

Arora, M. R. & Kelly, R. (1977). Some Aspects of the Anodic Oxidation of V, Mo, and W. *Journal of the Electrochemical Society*, *124*(10), 1493–1499. https://doi.org/10.1149/1.2133099.

Arshad, M. H., Wu, M., Saxena, K. K., Qian, J., Huang, S., & Reynaerts, D. (2022). Experimental investigations into machining characteristics of niobium carbide cermet with μECM/hybrid laser-μECM. *Procedia CIRP*, *113*, 385–391. https://doi.org/10.1016/j.procir.2022.09.188.

Aseerullah, M., Bhushan, C., & Vishwakarma, R. (2022). Analysis of CNC turning process of AA6082-T6 using Ansys software. In *2022 International Conference on Advances in Mechanical Engineering*, *1259*. https://doi.org/10.1088/1757-899X/1259/1/012017.

Awaludin, A. I. B., Tomadi, S. H., Rosdi, D., & Mas Ayu, H. (2022). Analysis and Simulation of Temperature Distribution and Stress Development in Wire EDM of Tungsten Carbide. *In 2021 3rd International Conference on Emerging Electrical Energy, Electronics and Computing Technologies*, *2312*. https://doi.org/10.1088/1742-6596/2312/1/012046.

Bannard, J. (1977). Electrochemical machining. *Journal of Applied Electrochemistry*, *7*(1), 1–29.

Bard, A. J., & Faulkner, L. R. (1980). Electrochemical methods: fundamentals and application. USA: John Wiley & Sons.

Blau, P. (2003). *Wear of materials*. USA: Elsevier.

Bozzini, B., De Gaudenzi, G.P., Fanigliulo, A, & Mele, C. (2003). Anodic behaviour of WC-Co type hardmetal. *Materials and Corrosion*, *54*(5), 295–303. https://doi.org/10.1002/maco.200390068.

Burov, V. G., Yanpolskiy, V. V., & Rakhimyanov, K. K. (2016). Technological aspects of forming the surface microrelief of low-wear coatings after electro-diamond grinding. *In 2015 VII International Scientific and Practical Conference on Innovations in Mechanical Engineering*, *126*. https://doi.org/10.1088/1757-899X/126/1/012018.

Cafe, R.F. (n.d.). Velocity of Sound in Various Media. RF Cafe. Retrieved from: https://www.rfcafe.com/references/general/velocity-sound-media.htm

Cardarelli, F. (2001). Materials Handbook — A concise desktop reference: Pub 2000. *Materials & Design, 22*(3), 237. https://doi.org/10.1016/s0261-3069(00)00075-3.

Ceratizit. (n.d.). Special Grade Data Sheet CTM12A

Chang, D. H. & Hung, J. C. (2011). Fabrication of fuel cells with high power density using micro electrical discharge machining milling. *Advanced Materials Research*, *335–336*, 1237–1241. https://doi.org/10.4028/www.scientific.net/AMR.335-336.1237.

Choi, S. H., Kim, B. H., Shin, H. S., Chung, D. K., & Chu, C. N. (2013). Analysis of the electrochemical behaviors of WC–Co alloy for micro ECM. *Journal of Materials Processing Technology*, *213*(4), 621–630. https://doi.org/10.1016/j.jmatprotec.2012.10.018.

Choi, S. H., Ryu, S.H., Choi, D.K., & Chu, C.N. (2006). Fabrication of WC micro-shaft by using electrochemical etching. *International Journal of Advanced Manufacturing Technology*, *31*, 682–687. https://doi.org/10.1007/s00170-005-0241-4.

Datta, M. (1993). Anodic dissolution of metals at high rates. *IBM Journal of Research and Development*, *37*(2), 207–226.

Davydov, A., & Kozak, E. (1990). *High-speed electrochemical machining (in Russian)*. Russia: Izd Nauk.

Davydov, A. D., Kabanova, T. B., & Volgin, V. M. (2017). Electrochemical machining of titanium. Review. *Russian Journal of Electrochemistry*, *53*, 941–965. https://doi.org/10.1134/S102319351709004X.

Davydov, A. D., Volgin, V. M., & Lyubimov, V. V. (2004). Electrochemical machining of metals: fundamentals of electrochemical shaping. *Russian Journal of Electrochemistry*, *40*, 1230–1265.

De Barr, A. E. & Oliver, D. A. (1968). *Electrochemical machining*. USA: American Elsevier Pub. Co.

Dutta, P., Barman, A., Kumar, A., & Das, M. (2020). Design and fabrication of electrochemical micromachining (ECMM) experimental setup for micro-hole drilling. *Advances in Mechanical Engineering*, 561–573. https://doi.org/10.1007/978-981-15-0124-1_51.

Egashira, K., Hayashi, A., Hirai, Y., Yamaguchi, K., & Ota, M. (2018). Drilling of microholes using electrochemical machining. *Precision Engineering*, *54*, 338–343. https://doi.org/10.1016/j.precisioneng.2018.07.002.

Ettmayer, P., & Walter Lengauer. (1994). *Carbides: Transition metal solid state chemistry encyclopedia of inorganic chemistry*. USA: John Wiley & Sons.

Fan, Z. W., & Hourng, L. W. (2011). Electrochemical micro-drilling of deep holes by rotational cathode tools. *International Journal of Advanced Manufacturing Technology*, *52*, 555–563. https://doi.org/10.1007/s00170-010-2744-x.

Fan, Z. W., Hourng, L. W, & Lin, M. Y. (2012). Experimental investigation on the influence of electrochemical micro-drilling by short pulsed voltage. *International Journal of Advanced Manufacturing Technology*, *61*, 957–966. https://doi.org/10.1007/s00170-011-3778-4.

Fan, Z. W., & Hourng, L. W. (2009). The analysis and investigation on the microelectrode fabrication by electrochemical machining. *International Journal of Machine Tools and Manufacture*, *49*(7-8), 659–666. https://doi.org/10.1016/j.ijmachtools.2009.01.011.

Feng, M., Xi, X. L., Zhang, L. W., & Nie, Z. R. (2022). Valence and coordination form transition of tungsten ions in molten alkali chlorides. *Physical Chemistry Chemical Physics*, *24*(34), 20130–20137. https://doi.org/10.1039/d2cp01359b.

Gao, C., Liu, Z., & Li, A. (2014). Study of micro drilling on pyrex glass using spark assisted chemical engraving. *Micro and Nanosystems*, *6*(1), 26–33. https://doi.org/10.2174/1876402905666131112201358.

Gattu, S. D., & Yan, J. (2022). Micro electrical discharge machining of ultrafine particle type tungsten carbide using dielectrics mixed with various powders. *Micromachines*, *13*(7). https://doi.org/10.3390/mi13070998.

Geethapriyan, T., Thulasikanth, V., Singh, V., Arun Raj, A. C., Lakshmanan, T., & Chaudhury, A. (2019). Performance characteristics of electrochemical micro machining of tungsten carbide. *Materials Today: Proceedings, 27*(3), 2381–2384. https://doi.org/10.1016/j.matpr.2019.09.134.

Göhr, H. (1966). Über anodisch gebildete oxidische deckschichten auf kobalt in wässeriger Lösung—I. Zur thermodynamik des systems kobalt-wässerige lösung (in German). *Electrochimica Acta, 11*(7), 827–834.

Goto, A., Nakata, A., & Saito, N. (2016). Study on Electrochemical Machining of Sintered Carbide. *Procedia CIRP*, *42*, 402–406. https://doi.org/10.1016/j.procir.2016.02.221.

Groover, M. P. (2020). *Fundamentals of modern manufacturing materials, processesand systems*. USA: John Wiley & Sons.

Hackert, M., Meichsner, G., Jahn, S. F. & Schubert, A. (2010). Investigating the influence of dynamic jet shapes on the jet electrochemical machining process. In *Proceedings of the Fourth European COMSOL Conference*.

Hackert, M., Meichsner, G., & Schubert, A. (2007). Electrochemical machining of carbide metal micro tools. In *7th EUSPEN International Conference, Nanotechnology*, *2*, 509–512.

Hackert-Oschätzchen, M., Martin, A., Kühn, R., Meichsner, G., Zinecker, M., & Schubert, A. (2013a). Micro-patterning of hard metals by electrochemical machining using closed-loop jet-Part 1. *Galvanotechnik*, *104*, 1133–1144.

Hackert-Oschätzchen, M., Martin, A., Kühn, R., Meichsner, G., Zinecker, M., & Schubert, A. (2013b). Micro-patterning of hard metals by electrochemical machining using closed-loop jet - Part 2. *Galvanotechnik*, *104*, 1308–13021.

Hackert-Oschätzchen, M., Martin, A., Meichsner, G., Zinecker, M., & Schubert, A. (2013c). Microstructuring of carbide metals applying jet electrochemical machining. *Precision Engineering*, *37*(3), 621–634. https://doi.org/10.1016/j.precisioneng.2013.01.007.

Hackert-Oschätzchen, M., Meichsner, G., Zinecker, M., Martin, A., & Schubert, A. (2012). Micro machining with continuous electrolytic free jet. *Precision Engineering*, *36*(4), 612–619. https://doi.org/10.1016/j.precisioneng.2012.05.003.

Hammer, C., Walther, B.. Karabulut, H., & Lohrengel, M. M. (2011). Oscillating oxygen evolution at Ta anodes. *Journal of Solid State Electrochemistry*, *15*, 1885–1891. https://doi.org/10.1007/s10008-010-1207-5.

Han, W., & Kunieda, M. (2017). Fabrication of tungsten micro-rods by ECM using ultra-short-pulse bipolar current. *CIRP Annals*, *66*(1), 193–196. https://doi.org/10.1016/j.cirp.2017.04.131.

Han, W., & Kunieda, M. (2018). Wire electrochemical grinding of tungsten micro-rods using neutral electrolyte.

Precision Engineering, *52*, 458–468. https://doi.org/10.1016/j.precisioneng.2018.02.006.

Harugade, M., Waigaonkar, S., Mane, N., & Hargude, N. (2019). Experimental investigation of high speed tool rotation on heat affected zone and over cut in ECDM. *Materials Today: Proceedings*, *18*, 1472–1478. https://doi.org/10.1016/j.matpr.2019.06.616.

Helmenstine, A. M.. (n.d.). Tungsten or wolfram facts. Retrived from chemistry.about.com

Hizume, S., & Natsu, W. (2021). Mechanism clarification and realization of scanning electrochemical machining of titanium alloys. *Journal of Advanced Mechanical Design, Systems, and Manufacturing*, *15*(5), JAMDSM0055. https://doi.org/10.1299/jamdsm.2021jamdsm0055.

Hochstrasser-Kurz, S. (2006). *Mechanistic study of the corrosion reactions on wc-co hardmetal in aqueous solution - an investigation by electrochemical methods and elemental solution analysis*. Doctoral thesis, Swiss Federal Institute of Technology.

Hung, J. C., Ku, C. Y., Der, G. M., & Fen, Z. W. (2016). Fabrication of an electrode insulation layer for electrochemical machining by using hot dip aluminizing and micro-arc oxidation method. *Procedia CIRP*, *42*, 390–395. https://doi.org/10.1016/j.procir.2016.02.217.

Hung, J. C., Yang, T. C., & Li, K. C. (2011). Studies on the fabrication of metallic bipolar plates - Using micro electrical discharge machining milling. *Journal of Power Sources*, *196*(4), 2070–2074. https://doi.org/10.1016/j.jpowsour.2010.10.001.

Hung, J.C., Ku, C.Y., & Fan, Z.W. (2018) Fabrication of an electrode insulated by using hot dip aluminizing and micro-arc oxidation method for electrochemical microhole machining. *Procedia CIRP*, *68*, 438–443. https://doi.org/10.1016/j.procir.2017.12.092.

Jacobs, L., Hyland, M. M., & De Bonte, M. (1998). Comparative study of WC-cermet coatings sprayed via the HVOF and the HVAF Process. *Journal of Thermal Spray Technology*, *7*, 213–218. https://doi.org/10.1361/105996398770350954.

Jahan, M. P. , Wong, Y. S., & Rahman, M. (2009). A study on the fine-finish die-sinking micro-EDM of tungsten carbide using different electrode materials. *Journal of Materials Processing Technology*, *209*(8), 3956–3967. https://doi.org/10.1016/j.jmatprotec.2008.09.015.

Joseph, X. B., Sherlin, V. A., Wang, S. F., & George, M. (2022). Integration of iron-manganese layered double hydroxide/tungsten carbide composite: An electrochemical tool for diphenylamine H(•+) analysis in environmental samples. *Environmental Research*, *212*. https://doi.org/10.1016/j.envres.2022.113291.

Kalra, C. S., Kumar, V., & Manna, A. (2020). Experimental study on developed electrochemical micro machining of hybrid MMC. *Indian Journal of Engineering and Materials Sciences*, *27*(3), 579–589. https://doi.org/10.56042/ijems.v27i3.45055.

Kamaraj, A. B., Dyer, R., & Sundaram, M. M. (2012). Pulse electrochemical micromachining of tungsten carbide. In *ASME 2012 International Manufacturing Science and Engineering Conference*, 415–421. https://doi.org/10.1115/MSEC2012-7238.

Károly, Z., & Szépvölgyi, J. (2005). Plasma spheroidization of ceramic particles. *Chemical Engineering and Processing: Process Intensification*, *44*(2), 221–224. https://doi.org/https://doi.org/10.1016/j.cep.2004.02.015.

Kellner, F. J. J., Hildebrand, H., & Virtanen, S. (2009). Effect of WC grain size on the corrosion behavior of WC-Co based hardmetals in alkaline solutions. *International Journal of Refractory Metals and Hard Materials*, *27*(4), 806–812. https://doi.org/10.1016/j.ijrmhm.2009.02.004.

Khalil, N., & Leach, J. S. L. (1986). The anodic oxidation of valve metals-I. Determination of ionic transport numbers by α-spectrometry. *Electrochimica Acta*, *31*(10), 1279–1285. https://doi.org/10.1016/0013-4686(86)80148-7.

Kittel, C., & McEuen, P. (1996). *Introduction to solid state physics*. USA: John Wiley & Sons..

Kleinhenz, S., Pfennig, V., & Seppelt, K. (1998). Preparation and structures of [W (CH3) 6], [Re (CH3) 6], [Nb (CH3) 6]−, and [Ta (CH3) 6]−. *Chemistry: A European Journal*, *4*(9), 1687–1691.

Kode, S. K., Ellis, J.D., & Mohammadi, H. (2022). Laser assisted diamond turning of tungsten carbide and the material properties required to obtain optical surface finish suitable for lens molds. In *2022 Polymer Optics and Molded Glass Optics: Design, Fabrication, and Materials*, 28–32. https://doi.org/10.1117/12.2635954.

Kokulnathan, T., Wang, T. J., Ahmed, F., & Alshahrani, T. (2023). Hydrothermal synthesis of ZnCr-LDH/Tungsten carbide composite: A disposable electrochemical strip for mesalazine analysis. *Chemical Engineering Journal, 451*. https://doi.org/https://doi.org/10.1016/j.cej.2022.138884.

Koyano, T., & Kunieda, M. (2013). Micro electrochemical machining using electrostatic induction feeding method. *CIRP Annals*, *62*(1), 175–178. https://doi.org/10.1016/j.cirp.2013.03.107.

Krüger, L., Mandel, K., Mandel, M., & Henschel, S. (2011). Field assisted sintering of ultrafine grained tungsten carbide cobalt and related mechanical and electrochemical properties. In *2011 European PM Conference Proceedings*, 1–5.

Kumar, A., Singh, A., Yadav, H. N. S., Kumar, M., & Das, M. (2021). 3D simulation of machining parameters of electrochemical micromachining for stainless steel (316L). *Materials Today: Proceedings*, *45*, 4565–4570. https://doi.org/10.1016/j.matpr.2021.01.005.

Kurlov, A. S., & Gusev, A. I. (2013). Tungsten carbides: structure, properties and application in hardmetals. Switzerland: Springer. https://doi.org/10.1007/978-3-319-00524-9.

Lackner, A., & Filzwieser A. (2002). Gas carburizing of tungsten carbide (WC) powder. *U.S. Patent*, 6,447,742

Li, W., Zhang, Y., & Song, X. (2011). The study of electrochemical polishing HVOF spraying coating. *Solid State Phenomena*, *175*, 259–262. https://doi.org/10.4028/www.scientific.net/SSP.175.259.

Lim, Y. M., & Kim, S. H. (2001). An electrochemical fabrication method for extremely thin cylindrical micropin. *International Journal of Machine Tools and Manufacture*, *41*(15), 2287–2296. https://doi.org/10.1016/S0890-6955(00)00129-2.

Lin, M. Y., Tsai, T. H., Hourng, L. W., & Wang, W. K. (2019). The effects of magnetic field and ethanol addition on the electrochemical discharge machining. *International Journal of Advanced Manufacturing Technology*, *105*, 2461–2467. https://doi.org/10.1007/s00170-019-04413-7.

Liu, Z., Nouraei, H., Spelt, J. K., & Papini, M. (2015). Electrochemical slurry jet micro-machining of tungsten carbide with a sodium chloride solution. *Precision Engineering*, *40*, 189–198. https://doi.org/10.1016/j.precisioneng.2014.11.009.

Lohrengel, M. M., Rataj, K. P., Schubert, N., Schneider, M., Höhn, S., Michaelis, A, … Schubert, A. (2014). Electrochemical machining of hard metals - WC/Co as example. *Powder Metallurgy*, *57*(1), 21–30. https://doi.org/10.1179/1743290113Y.0000000062.

Lohrengel, M. M., & Rosenkranz, C. (2005). Microelectrochemical surface and product investigations during electrochemical machining (ECM) in NaNO3. *Corrosion Science*, *47*(3), 785–794. https://doi.org/10.1016/j.corsci.2004.07.023.

Maeda, S., Saito, N., & Haishi, Y. (1967). Principle and characteristics of electro-chemical machining. *Mitsubishi Denki Giho*, *41*(10), 1267–1279.

Mahesh, K., Philip, J. T., Joshi, S. N., & Kuriachen, B. (2021). Machinability of Inconel 718: A critical review on the impact of cutting temperatures. *Materials and Manufacturing Processes*, *36*(7), 753–791. https://doi.org/10.1080/10426914.2020.1843671.

Martin, A., Eckart, C., Lehnert, N., Hackert-Oschätzchen, M., & Schubert, A. (2016). Generation of Defined Surface Waviness on Tungsten Carbide by Jet Electrochemical Machining with Pulsed Current. *Procedia CIRP*, *45*, 231–234. https://doi.org/10.1016/j.procir.2016.02.076.

Masuzawa, T. (2000). State of the art of micromachining. *CIRP Annals*, *49*(2), 473–488. https://doi.org/10.1016/S0007-8506(07)63451-9.

Masuzawa, T., Fujino, M., Kobayashi, K., Suzuki, T., & Kinoshita, N. (1985). Wire Electro-Discharge Grinding for Micro-Machining. *CIRP Annals*, *34*(1), 431–434. https://doi.org/10.1016/S0007-8506(07)61805-8.

Masuzawa, T., & Kimura, M. (1991). Electrochemical surface finishing of tungsten carbide alloy. *CIRP annals 40*(1), 199–202. https://doi.org/10.1016/S0007-8506(07)61967-2.

McGeough, J. A. (1974). *Principles of electrochemical machining*. UK: Chapman & Hall.

Mithu, M. A. H, Fantoni, G., & Ciampi, J. (2011). The effect of high frequency and duty cycle in electrochemical microdrilling. *International Journal of Advanced Manufacturing Technology 55*, 921–933. https://doi.org/10.1007/s00170-010-3123-3.

Muller, E. W., & Tsong, T. T. (1969). *Field Ion Microscopy: Principles and Applications*. USA: Elsevier.

Münninghoff, M. M. (2011). On the fundamental interface kinetics during ECM. *In 2011 International Symposium on Electrochemical Machining Technology*, 10–11.

Nakajima, H., Kudo, T., & Mizuno, N. (1999). Reaction of metal, carbide, and nitride of tungsten with hydrogen peroxide characterized by 183W Nuclear magnetic resonance and Raman spectroscopy. *Chemistry of Materials*, *11*(3), 691–697. https://doi.org/10.1021/cm980544o.

Natsu, W., Ikeda, T., & Kunieda, M. (2007). Generating complicated surface with electrolyte jet machining. *Precis Engineering*, *31*(1), 33–*39*. https://doi.org/10.1016/j.precisioneng.2006.02.004.

Natsu, W., & Kurahata, D. (2013). Influence of ECM pulse conditions on WC alloy micro-pin fabrication. *Procedia CIRP*, *6*, 401–406. https://doi.org/10.1016/j.procir.2013.03.093.

Natsu, W., Ooshiro, S., & Kunieda, M. (2008). Research on generation of three-dimensional surface with micro-electrolyte jet machining. *CIRP Journal of Manufacturing Science and Technology*, *1*(1), 27–34. https://doi.org/10.1016/j.cirpj.2008.06.006.

Nerz J., Kushner B., & Rotolico A. (1992). Microstructural evaluation of tungsten carbide-cobalt coatings. *Journal of Thermal Spray Technology*, *1*, 147–152. https://doi.org/10.1007/BF02659015.

Novikov, N. V., & Gurvich, R. A. (2003). On the effective power in electrolytic diamond machining of cemented carbides with polycrystalline cathodes. *Elektronnaya Obrabotka Materialov*, 4–11.

Palani, S., Lakshmanan, P., Arumugam, A., & Kulothungan, S. (2021). Experimental investigations of suitability of electrolyte solutions for anodic dissolution of nickel aluminum bronze. *Materials Today: Proceedings*, *46*, 966–971. https://doi.org/10.1016/j.matpr.2021.01.109.

Palani, S., Lakshmanan, P., & Kaliyamurthy, R. (2020) Experimental investigations of electrochemical micromachining of nickel aluminum bronze alloy. *Materials and Manufacturing Processes*, *35*(16), 1860–1869. https://doi.org/10.1080/10426914.2020.1813888.

Pierson, H. O. (1999). Handbook of chemical vapor deposition (CVD) - principles, technology, and applications. USA: William Andrew Publishing.

Pillai, H.P., Sampath, S.C., Elumalai, R., Hariharan, S., & Natarajan, Y. (2017) Influence of process parameters on electrochemical micromachining of Nimonic 75 alloy. *In ASME International Mechanical Enginerring Congress and Exposition. 58356, V002T02007*. https://doi.org/10.1115/IMECE2017-71147.

Pohanish R. P. (2012). *Sittig's handbook of toxic and hazardous chemicals and carcinogens.* USA: William Andrew. https://doi.org/10.1016/C2009-0-64361-0.

Pourbaix, M. (1974). *Atlas of electrochemical equilibria in aqueous solutions*. USA: National Association of Corrosion.

Qu, N. S., Zhang, Q. L., Fang, X. L., Ye, E. K., & Zhu, D. (2015). Experimental investigation on electrochemical grinding of inconel 718. *Procedia CIRP*, *35*, 16–19. https://doi.org/10.1016/j.procir.2015.08.055

Quarto, F. D., Paola, A. D., & Sunseri, C. (1980). Kinetics of growth of amorphous WO3 anodic films on tungsten. *Journal of the Electrochemical Society 127*, 1016–1021. https://doi.org/10.1149/1.2129809.

Rajurkar, K., Sundaram, M., & Malshe, A. (2013). Review of electrochemical and electrodischarge machining. *Procedia CIRP*, *6*, 13–26. https://doi.org/10.1016/j.procir.2013.03.002.

Rajurkar, K. P, Zhu, D., McGeough, J. A., Kozak, J., & De Silva, A. (1999). New developments in electro-chemical machining. *CIRP Annals*, *48*(2), 567–579. https://doi.org/10.1016/S0007-8506(07)63235-1.

Rataj, K. P. (2013). *Electrochemical characterization of technically relevant anodic oxide layers at low and high current densities.* Doctoral Dissertation, Heinrich Heine University.

Ratnasingam, J., Pew Ma, T., Ramasamy, G., & Manikam, M. (2009). The wear characteristics of cemented tungsten carbide tools in machining oil palm empty fruit bunch particleboard. *Journal of Applied Science*, *9*(18), 3397–3401. https://doi.org/10.3923/jas.2009.3397.3401.

Ratnasingam, J., Pew Ma, T., & Ramasamy, G. (2010). Tool temperature and cutting forces during the machining of particleboard and solid wood. *Journal of Applied Science*, *10*(22), 2881–2886. https://doi.org/10.3923/jas.2010.2881.2886.

Rudy, E., & Benesovsky, F. (1962). Untersuchungen in system tantal-wolfram-kohlenstoff. (in German). *Monatshefte Für Chemie Und Verwandte Teile Anderer Wissenschaften*, *93*, 1176–1195.

Sabahi, N., & Razfar, M. R. (2018) Investigating the effect of mixed alkaline electrolyte (NaOH + KOH) on the improvement of machining efficiency in 2D electrochemical discharge machining (ECDM). *International Journal of Advanced Manufacturing Technology, 95*, 643–657. https://doi.org/10.1007/s00170-017-1210-4.

Sara, R. V. (1965). Phase Equilibria in the system tungsten—carbon. *Journal of the American Ceramic Society, 48*(5), 251–257.

Schubert, N., Schneider, M., & Michaelis, A. (2011). Investigation of anodic dissolution of cobalt in alkaline solution. In *2011 7th International Symposium on Electrochemical Machining Technology.*

Schubert, N., Schneider, M., & Michaelis, A. (2014). Electrochemical Machining of cemented carbides. *International Journal of*

Refractory Metals and Hard Materials, 47, 54–60. https://doi.org/10.1016/j.ijrmhm.2014.06.010.

Schubert, N., Schneider, M., Michaelis, A., Manko, M., & Lohrengel, M. M. (2018). Electrochemical machining of tungsten carbide. *Journal of Solid State Electrochemistry, 22*, 859–868. https://doi.org/10.1007/s10008-017-3823-9.

Schubert, N., Schneider, M., & Michealis, A. (2013). The mechanism of anodic dissolution of cobalt in neutral and alkaline electrolyte at high current density. *Electrochimica Acta, 113*, 748–754. https://doi.org/10.1016/j.electacta.2013.06.093.

Schuster, R., Kirchner, V., & Allongue, P. (2000). Electrochemical micromachining. *Science*, *289*(5476), 98–101. https://doi.org/10.1126/science.289.5476.98.

Scopus. (n.d). Scopus. Retrieved from https://www.scopus.com/term/analyzer.uri?sid=3eaced6f1a6e1873d3434faee26e8ba6&origin=resultslist&src=s&s=%28TITLE-ABS-KEY%28%22electrochemical+machining%22+OR+ecm%29+AND+TITLE-ABS-KEY%28%22TUNGSTEN+CARBIDE%22+OR+WC%29%29&sort=plf-f&sdt=b&sot=b&sl=95&count=65&analyzeResults=Analyze+results&txGid=5dd9e136e94603904354dfd48ed14932

Sethi, A., Acharya, B.R., & Saha, P. (2022). Electrochemical dissolution of WC-Co Micro-Tool in Micro-WECM Using an eco-friendly citric acid mixed NaNO 3 electrolyte. *Journal of the Electrochemical Society, 169*(3), 033503. https://doi.org/10.1149/1945-7111/ac54d9.

Shamli, C. S., Hariharan, P., Yuvaraj, N., & Rajkeerthi, E. (2020) Impact of electrical process parameters in electrochemical micromachining of nimonic 75 alloy. *International Journal of Vehicle Structures and Systems*, *12*(2), 197–200. https://doi.org/10.4273/ijvss.12.2.18.

Shibuya, N., Ito, Y., & Natsu, W. (2012). Electrochemical machining of tungsten carbide alloy micro-pin with NaNO3 solution. *International Journal of Precision Engineering and Manufacturing*, *13*, 2075–2078. https://doi.org/10.1007/s12541-012-0273-2.

Shmanev, V. A, Filimoshin, V. G., & Karimov, A. K. (1986). *Tekhnologiya Elektrokhimicheskoy Obrabotki Detaley V Aviadvigatelestroenii (in Russian)*. Russia: Mashinostr Publishing

Sickafoose, S. M., Smith, A.W., & Morse, M. D. (2002). Optical spectroscopy of tungsten carbide (WC). *The Journal of Chemical Physics, 116*(3), 993–1002.

Sjöström, T., & Su, B. (2011). Micropatterning of titanium surfaces using electrochemical micromachining with an ethylene glycol electrolyte. *Materials Letters, 65*(23-24), 3489–3492. https://doi.org/10.1016/j.matlet.2011.07.103.

Song, K. S., & Williams, R. T. (1993). *Self-trapped excitons*. Germany: Springer. https://doi.org/10.1007/978-3-642-97432-8_7.

Song, K. Y., Chung, D. K., Park, M. S., & Chu, C. N. (2009). Micro electrical discharge drilling of tungsten carbide using deionized water. *Journal of Micromechanics and Microengineering*, *19*(4). https://doi.org/10.1088/0960-1317/19/4/045006.

Song, K. Y., Chung, D. K., Park, M. S., & Chu, C. N. (2010). Micro electrical discharge milling of WC-Co using a deionized water spray and a bipolar pulse. *Journal of Micromechanics and Microengineering*, *20*(4). https://doi.org/10.1088/0960-1317/20/4/045022.

Song, K. Y., Chung, D. K., Park, M. S., & Chu, C. N. (2012). Water spray electrical discharge drilling of WC-Co to prevent electrolytic corrosion. *International Journal of Precision Engineering and Manufacturing*, *13*, 1117–1123. https://doi.org/10.1007/s12541-012-0147-7.

Spieser, A., & Ivanov, A. (2015). Design of a pulse power supply unit for micro-ECM. *International Journal of Advanced Manufacturing Technology*, *78*, 537–547. https://doi.org/10.1007/s00170-014-6322-5.

Sun, Y., Deng, H., Liu, X., & Kang, X. (2022). Fabrication of tungsten tips with controllable shape by a two-step rapid reciprocating electrochemical etching method. *Review of Scientific Instruments*, *93*(12). https://doi.org/10.1063/5.0124438.

Sundaram, M. M., & Rajurkar, K.P. (2010). Electrical and electrochemical processes. In W. Zhang (Eds.), *Intelligent energy field manufacturing and interdisciplinary process innovations* (pp. 173–212). CRC Press. https://doi.org/10.1201/EBK1420071016.

Thakur, A., Tak, M., & Mote, R. G. (2019) Electrochemical micromachining behavior on 17-4 PH stainless steel using different electrolytes, *Procedia Manufacturing*, *34*, 355–361. https://doi.org/10.1016/j.promfg.2019.06.177.

Truckenbrodt, E. (1996). *Fluidmechanik*. Germany: Springer.

Walther, B., Schilm, J., Michaelis, A., & Lohrengel, M. M. (2007). Electrochemical dissolution of hard metal alloys. *Electrochimica Acta*, *52*(27), 7732–7737. https://doi.org/10.1016/j.electacta.2006.12.038.

Wang, F., Zhou, J., Wu, S., Kang, X., Gu, L., & Zhao, W. (2022). Material removal mechanism in photocatalytic-assisted jet electrochemical machining of SiC(p)/Al. *Micromachines*, *13*(9), 1482. https://doi.org/10.3390/mi13091482.

Wang, J., Xu, Z., & Zhu, D. (2023). Improving profile accuracy and surface quality of blisk by electrochemical machining with a micro inter-electrode gap. *Chinese Journal of Aeronautics*, *36*(4), 523–537. https://doi.org/10.1016/j.cja.2022.07.005.

Wang, S., Goto, A., & Nakata, A. (2017) Prevention of Material Deterioration in ECM of Sintered Carbide with Iron Ions (2 nd Report). *International Journal of Automation Technology*, *11*(5), 829–834. https://doi.org/10.20965/ijat.2017.p0829.

Wang, S., Goto, A., Nakata, A., Hayakawa, K., & Sakai, K. (2019). Recovery of sintered carbide material in electrochemical machining process. In *2018 17th International Conference on Global Research and Education*, 11–19. https://doi.org/10.1007/978-3-319-99834-3_2.

Wells, A. F. (2012). *Structural inorganic chemistry*. UK: Oxford University Press.

Wen, Z., Lu, D., Sun, J.,& Ji, S. (2011). *The Effect of Wc Doping on The Electrochemical Behavior of Nanosilicon/Cmc/Ab Composite Electrode. Advanced Materials Research*. 328–330, 1585–1588. https://doi.org/10.4028/www.scientific.net/AMR.328-330.1585.

Wilson, J. F. (1971). Practice and theory of electrochemical machining. USA: Wiley-Interscience.

Wu, Y. Y., & Sheu, D. Y. (2018) Investigating tungsten carbide micro-hole drilling characteristics by desktop micro-ECM with NaOH solution. *Micromachines*, *9*(10), 512. https://doi.org/10.3390/mi9100512.

Xu, L., Wang, J., & Zhao, C. (2023). Electrochemical micro-machining based on double feedback circuits. *Scientific Reports*, *13*(1), 1–11. https://www.nature.com/articles/s41598-022-25964-y.

Xue, J., Dong, B., & Zhao, Y. (2022). Significance of waveform design to achieve bipolar electrochemical jet machining of passivating material via regulation of electrode reaction kinetics.

International Journal of Machine Tools and Manufacture, *177*, 103886. https://doi.org/10.1016/j.ijmachtools.2022.103886.

Yamamura, K., Imanishi, Y., & Endo, K. (2016) Electrochemical mechanical polishing of difficult- To-machine mold materials. In *EUSPEN 2016 16th International Conference & Exhibition.*

Yan, M., Zhao, Z., Wang, T., Chen, R., Zhou, C., Qin, Y., . . . Yang, Y. (2022). Synergistic effects in Ultrafine Molybdenum–Tungsten Bimetallic Carbide hollow carbon architecture boost hydrogen evolution catalysis and lithium-ion storage. *Small*, *18*(37). https://doi.org/10.1002/smll.202203630.

Yang, C. K., Cheng, C. P., Mai, C. C., Wang, A. C., Hung, J. C., & Yan, B. H. (2010). Effect of surface roughness of tool electrode materials in ECDM performance. *International Journal of Machine Tools and Manufacture*, *50*(12), 1088–1096. https://doi.org/10.1016/j.ijmachtools.2010.08.006.

Yang, P. Z., Hung, J. C., & Cheng, C. W. (2017). Fabrication of tungsten carbide micro fins by sliding ECM. In *IEEE 2017 8th International Conference on MEchanical and Aerospace Engineering*. 136–139. https://doi.org/10.1109/ICMAE.2017.8038630.

Ye, L., Saxena, K. K., Huang, S., Qian, J., Vleugels, J., & Reynaerts, D. (2022). Experimental investigations on micro-EDM milling of niobium carbide-nickel based cermet using statistical and empirical techniques. *Procedia CIRP, 113*, 47–52. https://doi.org/10.1016/j.procir.2022.09.118.

Zhang, Q., Luo, H., Liu, P., Liu, G., & Zhang, Y. (2022). Bipolar nano-second pulse power supply for electrochemical micromachining of tungsten carbide without tool wear. *Procedia CIRP*, *113*, 471–476. https://doi.org/10.1016/j.procir.2022.09.202.

Zhang, X., Huang, R., Liu, K., Kumar, A. S., & Deng, H. (2018). Suppression of diamond tool wear in machining of tungsten carbide by combining ultrasonic vibration and electrochemical processing. *Ceramics International, 44*(4), 4142–4153. https://doi.org/10.1016/j.ceramint.2017.11.215.

Zhang, X. H., Wang, L., & Long, J. P. (2011). Effects of two-step DC electrochemical pretreatment of fine grinding WC-Co tool surface on morphology and quality of diamond coatings. *Advanced Materials Research*, *337*, 59–62. https://doi.org/10.4028/www.scientific.net/AMR.337.59.

Zhong, Y., & Shaw, L. (2011). A study on the synthesis of nanostructured WC–10 wt% Co particles from WO3, Co3O4, and graphite. *Journal of Materials Science, 46*, 6323–6331. https://doi.org/10.1007/s10853-010-4937-y.

Zhou, P. F., Xiao, D. H., & Yuan, T. C. (2017). Comparison between ultrafine-grained WC–Co and WC–HEA-cemented carbides. *Powder Metallurgy*, *60*(1), 1–6. https://doi.org/10.1080/00325899.2016.1260903.

How to Cite: Asmael, M. & Memarzadeh, A. (2024). A Review on Recent Achievements and Challenges in Electrochemical Machining of Tungsten Carbide. *Archives of Advanced Engineering Science,* 2(1), 1–23, https://doi.org/10.47852/bonviewAAES3202915